PREDICTION OF THE STATIC PRESSURE INDUCED BY A FOAM EARPLUG INSIDE A CYLINDRICAL EARCANAL

by

Seyed Saber SARRAF HOSSEINIAN

THESIS PRESENTED TO ÉCOLE DE TECHNOLOGIE SUPÉRIEURE
IN PARTIAL FULFILLMENT FOR A MASTER'S DEGREE
WITH THESIS IN MECHANICAL ENGINEERING
M.A.Sc.

MONTREAL, AUGUST 29, 2021

ÉCOLE DE TECHNOLOGIE SUPÉRIEURE
UNIVERSITÉ DU QUÉBEC

BOARD OF EXAMINERS

THIS THESIS HAS BEEN EVALUATED

BY THE FOLLOWING BOARD OF EXAMINERS

Mr. Eric Wagnac, Thesis Supervisor
Department of Mechanical Engineering, École de technologie supérieure

Mr. Franck Sgard , Thesis Co-supervisor
Scientific division, Institut de recherche Robert-Sauvé en santé et en sécurité du travail

Mrs. Nicola Hagemeister, Chair, Board of Examiners
Department of Systems Engineering, École de technologie supérieure

Mr. Olivier Doutres, Member of the jury
Department of Mechanical Engineering, École de technologie supérieure

THIS THESIS WAS PRENSENTED AND DEFENDED

IN THE PRESENCE OF A BOARD OF EXAMINERS AND PUBLIC

ON AUGUST 23, 2021

AT ÉCOLE DE TECHNOLOGIE SUPÉRIEURE

ACKNOWLEDGMENT

The endeavors of individuals who accompanied me during this research project are appreciated. Specially, endeavors of Prof. Eric Wagnac whom scientifically supported, the endeavors of Dr. Franck Sgard and his significant notations and financial support provided from IRSST, the facilities provided by Prof. Olivier Doutres which helped to progress this project, and the efforts of Ms. Elizabeth Laroche at Sacré-Coeur-de-Montreal Hospital to accomplish experimental tests results, are greatly appreciated.

PRÉVISION DE LA PRESSION STATIQUE INDUITE PAR UN BOUCHON D'OREILLE EN MOUSSE À L'INTÉRIEUR D'UN CANAL AURICULAIRE CYLINDRIQUE

MÉMOIRE

Seyed Saber SARRAF HOSSEINIAN

RESUME

Plus de 120 million de travailleurs dans le monde sont exposés à des niveaux de bruit dangereux. Chaque jour, 360000 travailleurs (Québec) sont exposés à des niveaux de bruit (90 dBA) pouvant entraîner une perte auditive. Une façon de protéger les travailleurs consiste à utiliser des protecteurs auditifs (PA). L'utilisation des PA n'est pas efficace pour les porteurs car ils sont souvent portés de manière incorrecte ou incohérente. La cause la plus importante est l'inconfort induit par les PA. Cette thèse fait partie d'un projet de recherche de grande ampleur et se concentre sur la prédiction de la pression mécanique statique (PMS) sur la paroi du canal auditif humain induite par un bouchon d'oreille en mousse, qui est l'une des sources d'inconfort évoquées dans la littérature. Il n'existe actuellement aucun banc d'essai pour mesurer la PMS à l'interface entre le bouchon d'oreille en mousse et le canal auditif humain. L'objectif principal de cette maîtrise est de concevoir des testeurs virtuels pour prédire la PMS exercée par un bouchon d'oreille en mousse inséré dans un canal auriculaire cylindrique simplifié. Les objectifs spécifiques visant à construire des modèles par éléments finis (MEF) avec deux niveaux de complexité: 1) Un modèle simulant l'insertion du bouchon d'oreille en mousse dans un canal auriculaire rigide simplifié de forme cylindrique sans couche de peau. 2) Un modèle qui simule l'insertion du bouchon d'oreille en mousse dans un canal auditif cylindrique qui comprend les tissus mous environnants (couches cutanées). Un bouchon d'oreille (3M Classic E.A.R en mousse CVP) est envisagé. Les propriétés mécaniques de la peau humaine ont été calibrées à partir d'essais tirés de la littérature alors que celles du bouchon d'oreille en mousse ont été obtenues d'essais de caractérisation. Le modèle avec conduit cylindrique rigide a été validé en comparant les résultats de simulation à

ceux d’une expérience réalisée dans des conditions similaires. Une très bonne corrélation fut obtenue à partir des résultats des tests de compression transversale et axiale du bouchon d'oreille en mousse en simulation expérimentale et numérique. Les courbes force-déplacement obtenues par simulation numérique de test d’indentation sur la peaur montrent une très bonne correspondance avec les données expérimentales tirées de la littérature. La force de contact entre le bouchon d'oreille en mousse et le canal auriculaire cylindrique rigide est mesurée par un test expérimental. Les simulations numériques sont effectuées pour imiter des tests expérimentaux. Les forces de contact calculées à l'interface entre le bouchon d'oreille en mousse et le canal auriculaire cylindrique rigide sont de 1,6 N sans couche de peau et de 1,5 N avec couche de peau. La PMS à l'interface entre le bouchon d'oreille en mousse et le canal auriculaire cylindrique rigide sans couche cutanée et avec couche cutanée est de 3,40 kPa et 3,18 kPa, respectivement.

Mots-clés: pression mécanique statique, équipement de protection auditive, problèmes de surdité, conduit auditif humain, peau humaine, bouchon d'oreille en mousse, méthode des éléments finis, modélisation 3D

DESIGN OF A VIRTUAL TESTER TO PREDICT STATIC MECHANICAL PRESSURE (SMP) INDUCED BY A FOAM EARPLUG INSIDE CYLINDRICAL EARCANAL

Seyed Saber SARRAF HOSSINIAN

ABSTRACT

Over 120 million workers across the globe are exposed to dangerous levels of noise. Daily, 360,000 workers (Quebec province) are exposed to noise levels (90 dBA) that could cause hearing loss. One way to protect workers is the usage of hearing protection devices (HPDs). The use of HPDs is not efficient for wearers because they are often worn incorrectly or inconsistently. The most significant cause is discomfort induced by HPDs. This thesis is part of large project and focused on the prediction of the static mechanical pressure (SMP) on human's earcanal wall induced by foam earplug, which is one of the sources of discomfort mentioned in the literatures. Currently, there is no available test bench or methods to measure the SMP at the interface between foam earplug and human earcanal. Accordingly, the main objective of this master thesis is to predict the SMP exerted by a foam earplug inserted into a simplified cylindrical earcanal. The specific objectives aimed at building finite element models (FEM) with two levels of complexity: 1) a model that simulates the insertion of the foam earplug in a simplified rigid earcanal of cylindrical shape without skin layer; 2) a model that simulates the insertion of the foam earplug in a more realistic earcanal that includes the surrounding soft tissue (skin layers). An earplug (3M classic E.A.R made of PVC foam) is considered. The mechanical properties of the human skin and foam earplug are characterized. The characterized mechanical properties of human skin and foam earplug were validated by using numerical simulation (FEM). A very good correlation is obtained from results of transverse and axial compression tests of foam earplug in both experimental and numerical simulation. The numerical simulation results for the force-displacement relationship obtained in indentation test on skin show a very good match with experimental data. The contact force between foam earplug and rigid cylindrical earcanal was measured by experimental test. The numerical simulations are carried out to mimic experimental tests. The contact forces were computed at the interface between the foam earplug and the rigid cylindrical earcanal was

approximately 1.6 N without a skin layer and 1.5 N with a skin layer. The SMP at the interface between the foam earplug and the rigid cylindrical earcanal were 3.40 kPa without a skin layer and 3.18 kPa with a skin layer.

Keywords: static mechanical pressure, hearing protection device, hearing loss issues, human earcanal, human skin, foam earplug, finite element method, 3D modeling

TABLE OF CONTENTS

Page

LIST OF TABLES

Page

LIST OF FIGURES

Page

LIST OF ABREVIATIONS

ANSI	American National Standards Institute
ASA	Acoustical Society of America
ATF	Acoustic Test Fixture
CT	Computed Tomography
DMA	Dynamic Mechanical Analysis
DMS	Dynamic Mechanical Spectrometry
FE	Finite Element
FEM	Finite Element Method
HPC	High Processing Computers
HPD	Hearing Protection Devices
MRI	Magnetic Resonance Imaging
NR	Noise Reduction
NRR	Noise Reduction Ratio
NSERC	Natural Sciences and Engineering Research Council of Canada
OHS	Occupational Health and Safety
PU	Polyurethane
PVC	Polymer vinyl chloride
QMA	Quasi-static Mechanical Analysis
SMP	Static Mechanical Pressure

LIST OF SYMBOLS

F_d	Downward force
F	Radial Force
Pa	Pressure unit over area (Pascal)
N	Force unit (Newton)
θ	Angle parameter
P	Expansion pressure
r	Earcanal radius
L	Earplug length
mV	Millivolt
mm Hg	Millimeter mercury
W	Strain energy function
C_j	Material constant
b_j	Material constant
n	Material constant
J	Deformation rate
μ	Shear modulus
K	Bulk modulus
ρ	Density
I_1	First invariant
C_{10}	New-Hookean parameter
t_i	Cauchy stress tensor

INTRODUCTION

One risk factor in workplace is definitely noise (Berger et. al, 2003). Daily, 360,000 workers in Quebec province are exposed to noise levels (90 dBA) that could cause hearing loss. Hearing loss in workplace is a significant issue. The reduction of noise at the source is the most appropriate solution to prevent employee hearing loss. Another way to protect workers is the usage of hearing protection devices (HPD). According to Quebec standards, a worker should not be exposed to more than 90 decibels for an eight-hour working shift. If the noise level increases by merely 5 dB, exposure time should be reduced by 50% (four hours). If noise reduction at the source or along the propagation path is not possible, workers must wear HPDs. In fact, the HPD acts as an acoustic barrier at the ear's entrance to block a certain amount of acoustic energy from the noisy environment. However, workers may wear HPDs incorrectly and intermittently. The most significant cause is discomfort induced by HPDs. Indeed, HPDs induce acoustical issues (e.g. attenuation and occlusion effects), physical issues (e.g. mechanical pressure exerted by the HPD on the ear tissues), functional issues (e.g. maintaining in position) and psychological discomforts (e.g. acceptability and habituation). Notably, the chronic noise exposure not only causes increase of stress, hypertension and blood pressure, but also reduction of the productivity and quality of life.

This master thesis project is part of an ongoing large research project that aims at developing tools to assist preventers in choosing the most appropriate HPDs accounting for their comfort and to help manufacturers designing earplugs that are more comfortable. The global objective of the project is to design virtual and experimental testers to evaluate HPDs comfort.

This master thesis project focuses on the numerical simulation of the static mechanical pressure (SMP) on human's earcanal wall induced by foam earplug. The SMP is one specific variable associated to the physical phenomena involved in the assessment of the biomechanical component of comfort and one of the sources of discomfort mentioned in the literature. The SMP, moreover, is involved in the functional component of comfort such as

annoyance, maintaining in position and difficulty of insertion. Currently, no test bench for measuring SMP is available. The development of such a test bench is a significant challenge given the geometric complexity of the earcanal and the available sensor technologies.

But what exactly is SMP? SMP is the result of the interaction between an earplug and the earcanal wall. Thus, it is directly related to the geometry and the material properties of the earplug and the earcanal. In other words, earplug induces a SMP on the earcanal wall and substructures (cartilage, soft tissues, skin and bone). This mechanical pressure can be defined as a contact pressure between two solids (skin and earplug).

The main objective of this dissertation is to create and validate a finite element model (FEM) that predicts the static mechanical pressure (SMP) exerted by a foam earplug inserted into a simplified cylindrical earcanal. To achieve the main objective, two specific objectives are considered: 1) A model that simulates the insertion of the earplug in a simplified rigid earcanal of cylindrical shape without skin layer and 2) a model that simulates the insertion of the earplug in a more realistic earcanal that includes the surrounding soft tissue (skin layer). The geometry of non-deformed earcanal will be based on a simplified cylindrical earcanal. The mechanical properties of the soft tissues (i.e. skin and substrate layers) within the earcanal will be calibrated from literature data while those of a foam earplug (i.e. 3M foam Classic) will be calibrated from in-house mechanical characterization. Experimental tests will be used to validate the numerical simulations. The scientific knowledge developed about deformation mechanism of earcanal skin and foam earplug will be improved. Ultimately, the virtual SMP tester will help earplug manufacturers to modify their products to increase their comfort. By improving the earplug comfort, hearing loss issues between workers are expected to be reduced.

This dissertation is divided into six chapters. In the first chapter, previous research works and literature review are debated. The second chapter is related to research problems and objectives. The third chapter is related to research methods while the fourth chapter presents

the results. In the fifth chapter, the discussion is presented. The manuscript ends with a conclusion and the perspectives of the project.

CHAPTER 1

LITERATURE REVIEW

This chapter will introduce the reader to the concepts necessary to better understand the context of this dissertation.

1.1 Anatomy of the hearing system

The human ear is constituted of three functional parts: the inner (internal) ear, the middle ear and the outer (external) ear. Each part consists of different organs with separate function. In Figure 1.1, a basic anatomy of the human ear is illustrated (Maroonroge et. al, 2000).

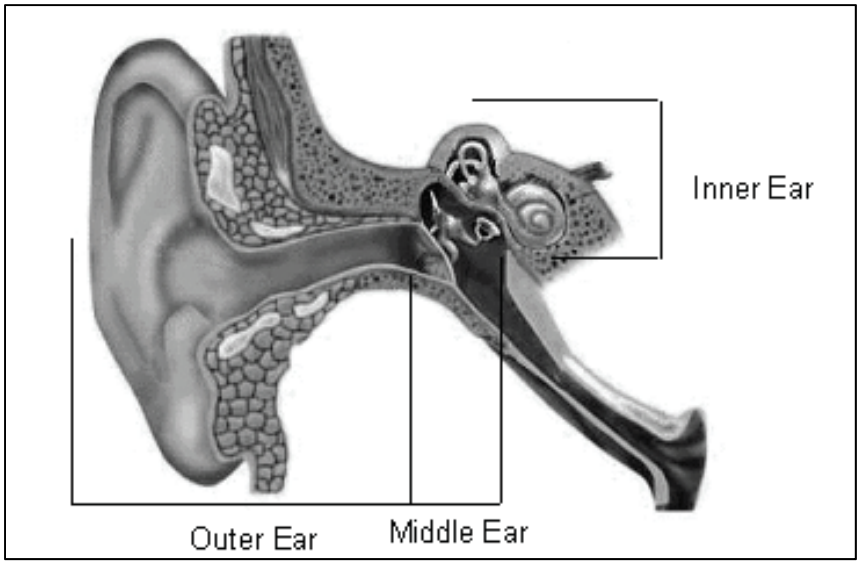

Figure 1.1 The structure of human ear

Taken from Maroonroge et al. (2000, p. 8)

The outer part of human ear includes two main sections called the pinna and the earcanal. The pinna is a structure consisting of an ellipsoidal geometry and uneven surface with channels. The inner structure of the pinna contains a single piece of cartilage attached to

surrounding tissues. The inner structure of the pinna is covered with skin. Actually, the earcanal is a conical duct, which begins at the lower part of the pinna (concha) and terminates at the eardrum, a tympanic membrane that separates the outer ear from the middle ear (Maroonroge et. al, 2000). The geometry of the earcanal is like the letter "S" with its two bends. The outer two thirds of the earcanal is surrounded by cartilage, while the remaining inner one third is surrounded by bone. The cartilaginous part is covered with a thick layer of skin (approximately 0.5 to 1.0 mm). The cartilaginous part is the continuation of the pinna and contains several sebaceous glands, wax, and hair. The osseous part of the earcanal is coated with relatively thin skin (0.2 mm). This part is continuous with the outer layer of the eardrum (Maroonroge et. al, 2000).

In adult males, the average length of the earcanal is about 25 mm, whereas the female's earcanal has a length of around 23 mm. The concha is attached to the earcanal, thus the effective length of the earcanal is longer than its real length. The cross-section shape of the earcanal is oval (7.0 - 8.0 mm, diameter) and changes along its length and reduces from entrance to eardrum. The isthmus is the narrowest section of the earcanal and is located after the second bend approximately 4 mm before the eardrum (Maroonroge et. al, 2000). The eardrum (see Figure 1.1) stands at a skew angle (45° to 60°).

1.2 Categories of hearing protection devices (HPDs)

The hearing protection devices can be categorized into three separate main groups, i) earplugs that are inserted into the earcanal, ii) earmuffs that shield the outer ear and the pinna, iii) helmets or *noise-canceling shells* that shield human's heads. In Figure 1.2, the typical HPDs and their classification are illustrated.

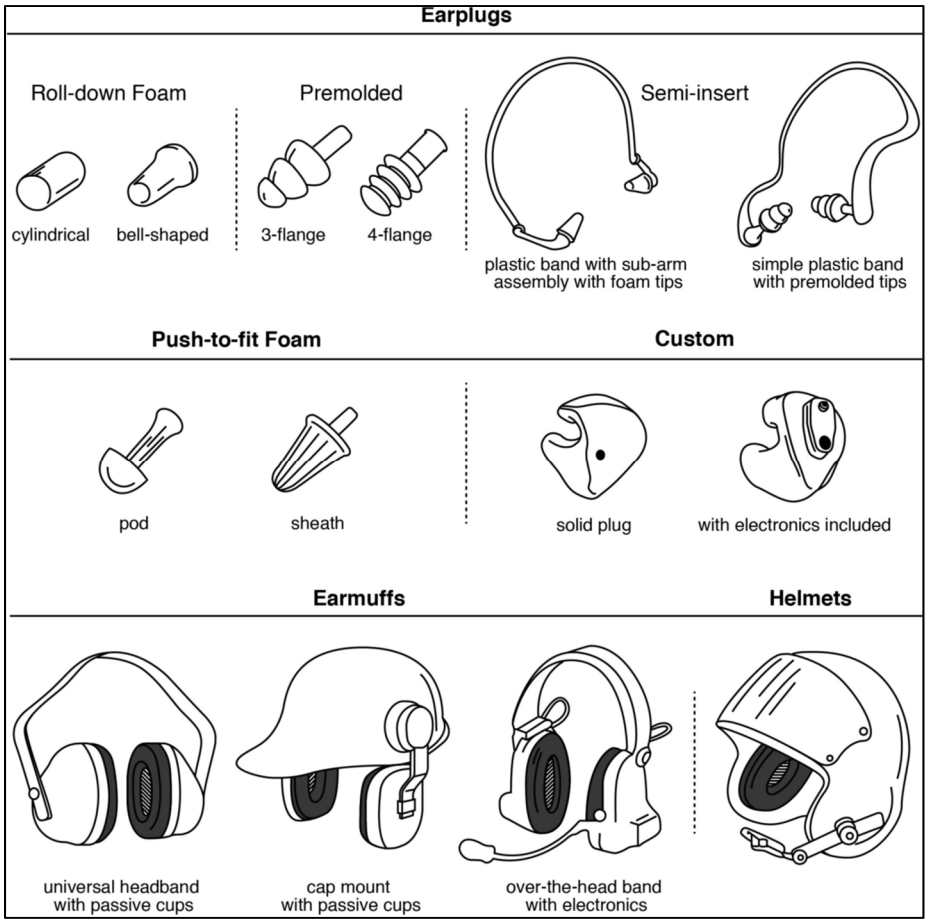

Figure 1.2 Typical HPDs and their classification

Taken from Voix et al. (2014, p. 2)

According to Figure 1.2, helmets are mostly used in workplaces or occupations, in which not only hearing loss can be an issue, but also protection of the head and the skull is required. For instance, helmets can be an appropriate protector in metal working factories, mining, and construction industries as well as for pilots, automobile drivers, motorcycle drivers and even welders.

Earmuffs can be divided into three sub-groups (see Figure 1.2); the universal headband with passive cups, cap mount with passive cups and headband with active electronics. Earplugs are manufactured in different shapes with various materials depending on their application. They are nominally divided into five sub-groups: roll-down foam, premolded, semi-insert,

push to fit foam and custom molded. The latter have more attenuation than other types of earplugs, because their shape is close to the geometry of the user's earcanal and they are produced with an *airtight seal* (Berger et. al, 2011). In fact, when custom earplug is deeply inserted beyond the earcanal's second bend, the maximum mitigation of noise can be obtained. However, this situation really depends on the specialist who fabricates the custom molded earplug (i.e. quality of the molding and the subsequent adjustment). It is noteworthy that custom molded earplug is not necessary the most comfortable one according to the literature.

It is evident that each kind of HPDs family has some benefits and drawbacks. Earplugs are the most commonly used protectors in the noisy environment. However, the protection prepared by the earplugs is known to be less reliable than earmuffs, because correctly positioning earplug in the earcanal is difficult. Therefore, earplugs are recommended for use over long working shift unlike earmuffs that can more easily be removed and reinstalled. Some types of earplugs are also known to cause excessive attenuation, which can overprotect the wearers. This overprotection prevents worker from communicating with colleagues and from hearing emergency acoustic signals. This dissertation focuses only on 3M classic foam earplug.

1.3 Definition of comfort dimensions

1.3.1 Components of comfort associated with earplugs and their attributes

The existing literature shows that the comfort is a feeling while wearing earplugs. Earplugs may vary by their geometry, the material, fit and usability (e.g. ease of insertion). The material includes mass, stiffness, thermal conductivity, texture etc. These design parameters affect the acoustical, mechanical, thermal and functional behaviors.

The comfort associated with wearing an earplug can be explained in three main components:
1) **The physical component** concerns the perception of the individual resulting from the interaction between the earplug and the earcanal, on an acoustic, biomechanical and thermal point of view. The acoustic subcomponent is associated with noise perception often

characterized by the following attributes: speech intelligibility, warning signals or machine noise audibility and occlusion effect. The biomechanical subcomponent is characterized by the static mechanical pressure exerted on the earcanal and pain or irritation induced by mechanical contact. The thermal subcomponent is related to the heating and sweating of the skin in the earcanal.

2) **The functional component** depends on the ergonomics of the earplug and its capacity to fulfill the objectives set for it. It is often characterized by the following attributes: usability of the earplug, convenience of use, ease of positioning and holding in position.

3) **The psychological component** relates, directly, to the user's feelings in the terms of acceptability of the earplug, habituation to the earplug, or satisfaction with it.

Furthermore, certain attributes of the physical and functional components of comfort are directly connected to the design parameters of the earplugs. The comfort attributes are controllable by the manufacturer such as over-attenuation, sub-attenuation, maintaining in position, irritation and static mechanical pressure. Some attributes of the psychological component may also depend on the design of the earplugs. For example, molded earplugs in the form of screws and nuts have been proposed to increase earplug acceptability in factories.

1.3.2 Biomechanical subcomponent of comfort

The main attributes for the biomechanical subcomponent of comfort are pain, static mechanical pressure (SMP) on human soft tissues (e.g. skin) and irritation (related to earplug texture). The mechanical pressure exerted by the earplug on the earcanal components (skin, soft tissues and bones) covers the physical variable that causes this discomfort (Gerges and Casali, 2007). The SMP is a characteristic of the tribological system "earcanal or earplug" and is therefore related to the geometrical and material properties of the earplug and the earcanal. (Zwislocki, 1985) mentioned that the SMP is the main source of discomfort, however it is also related to the effective attenuation of the earplug. He did not rely on subjective tests. He opposed comfort and attenuation through the sole pressure effects on the earcanal. He rose that just one acceptable answer (dependent on noise level) is available to

make a balance between both sound attenuation of earplug and its discomfort. People with earcanal pain problems are less likely to be wearing earplug. Irritation and pain of the earcanal during withdrawal of earplug are introduced in some publications. Irritation can logically be connected to the texture of the earplugs and accentuated by working conditions (e.g. heat or moisture). (Park & Casali, 1991) showed that the generic attribute “pain” is significantly correlated with the concept of comfort for the tested participants.

1.3.3 Functional component of comfort

The main generic attributes for the functional component of comfort are annoyance, maintaining in position and difficulty of insertion. (Coles and Rice, 1966) mentioned that the earplug considered to be the least comfortable and the least easy to wear, and having a tendency to fall. However, earplugs allow better intelligibility which highlights the trade-offs that may exist when evaluating comfort. The ease of installation is related to the ergonomic, geometric or material aspects, and is considered during the design of the earplug itself. Concerning the maintaining in position, (Sweetland et. al, 1983) insisted that it could be a remarkable factor in the estimation of comfort, especially in difficult working conditions. As for the convenience of installation, the maintaining in position will be connected as much to the geometry as to the chosen material or to the working conditions. The main reason of discomfort is the SMP. The SMP causes annoyance and irritation inside earcanal, therefore the SMP is involved in functional component of comfort. The SMP has a direct influence on annoyance. The higher SMP causes more annoyance for wearer.

1.4 Contact pressure on human skin

In real life, many situations can cause pain or discomfort for different organs of the human body. One type of discomfort is crouching and kneeling. The latter means that a part of the body (e.g. knee) has a bending position during working hours, causing blood flow reduction of blood flow and in long term, potential disorders. Another example could be a part of body (such as hand or feet) that accidentally impacts on a tough surface causing a contact pressure. The contact pressure of a sharp object on the skin will cause pain. Pain induced by contact pressure may also occur, for instance, when resting an arm on a desk for a long time when

sitting for a long time on a chair or when standing on feet for a long time without adequate movements (Albin et. al, 2007, Maquet et. al, 2004, & Kilbom et. al, 1993). Some considerable interesting conclusion can be derived from (Albin et. al, 2007). The external applied pressure causes deformation, blood flow reduction and changes in cellular structure on tissue. A pressure of 3.99 kPa exerted on capillaries can collapse them and produce an ischemic state. The effects of discomfort depend on the interaction between pressure magnitude and exposure time. Generally, contact pressures less than 3.99 kPa during 30-60 minutes exposure time are unlikely to cause pain.

1.5 What is static mechanical pressure (SMP) on earcanal wall?

The SMP is the result of the interaction between the earplug and the earcanal wall, thus it has direct relations to the geometry and the material properties of the earplug and the earcanal (Figure 1.3).

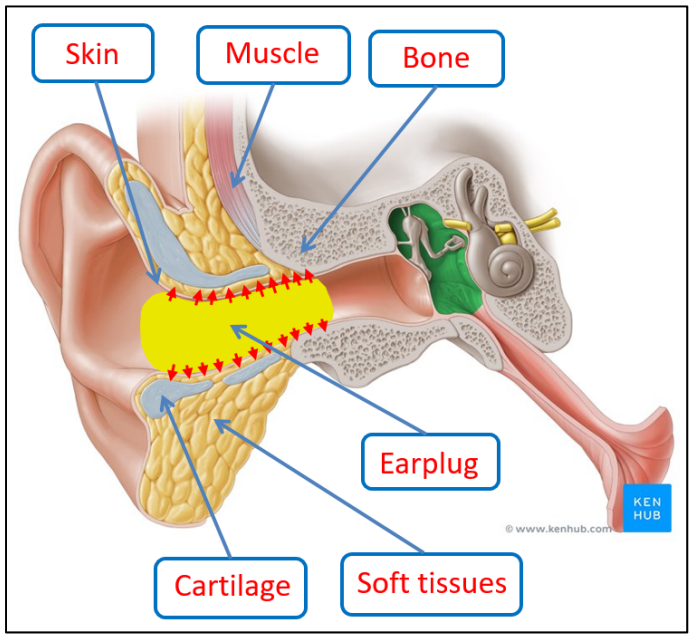

Figure 1.3 Static mechanical pressure (SMP) on earcanal wall
Taken from (www.kenhub.com)

According to Figure 1.3, it is evident that earplug induces the SMP on earcanal wall and substructures (cartilage, soft tissues, skin and bone). This mechanical pressure can be defined

as a contact pressure between two soft solids. The small red arrows demonstrate the SMP direction, which is distributed inconsistently on earcanal wall.

1.6 Numerical modeling for computation of the SMP

There is one published scientific articles about numerical simulation for computation of SMP on earcanal walls. Some researchers accomplished the computation of SMP on other human parts. The explanation of other body parts seems useless, because in this dissertation earcanal wall is the main subject for computation of SMP.

(Baker et. al, 2010) used numerical simulation to predict discomfort and the SMP of earplugs. In order to mimic real condition, the geometry of the human ear (the external ear and earcanal) was combined with the earplugs geometries. This combination was represented the induced stresses and strains during the insertion of earplug into the earcanal. The SMP between the two objects was predicted by numerical simulation. The output data was analyzed to estimate the SMP and discomfort. 3D scanning technologies were used to design geometries mimicking structures of human ear (external and internal). Multiple material layers were considered to simulate approximately the real layers of human ear skin. The insertion and stress relaxation of the earplugs were numerically simulated. The main objective of their work was evaluating the potential of using numerical simulation (solid mechanics) as a tool to predict the comfort of earplug designs (e.g. the SMP).

(Baker et. al, 2010) described that a combination of a number of features were required to create a model of the interaction between earplugs and a human ear. The numerical simulation of both the human ear and the earplug was required relevant material modeling. The material layers were simplified into two layers, a uniform skin material layer overlaying a base substrate. To represent the testing conditions used by (Tran et. al, 2007), a virtual test method was established. In the substrate material, the Young's modulus was modified until the resulting stress/strain curve was approximately near to experimental data of (Tran et. al, 2007) work. The obtained Young's modulus for skin layer and base substrate were equal to 5.67 kPa and 36.62 kPa, respectively. The obtained Poisson's ratios were equal to 0.48 and

0.42 for skin layer and base substrate, respectively. In Figure 1.4, the virtual test configuration is depicted, where the penetration depth (zero to 2 mm) was represented by ”h”. The sample (skin and substrate) size was square at 60 mm×60 mm with a thickness “t” equal to 20 mm (at least 10 times larger than the penetration depth). The radius of spherical indenter was equal to 6.22 mm.

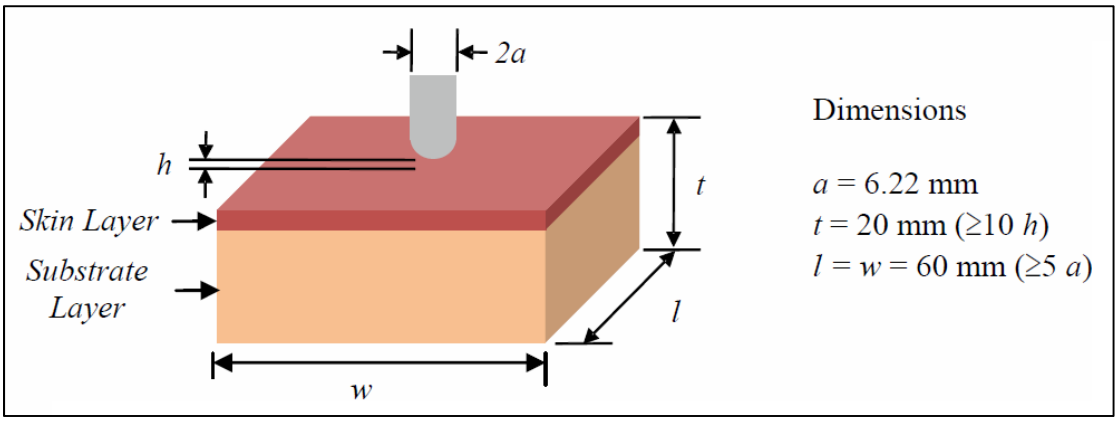

Figure 1.4 Virtual test model to represent indentation test method

Taken from Baker et al. (2010, p. 5)

The internal structure of the human ear was designed using ear impression. The ear impression scans were captured using the HD 3D scanner (NextEngine Inc. of Santa Monica, California). Three earcanal sizes (small, medium, and large) were selected. The aim of selecting three earcanal sizes was to create a uniform population between various earcanal geometries. The external structure of human ear was taken using the 3dMDTorso® equipment (3dMD of Atlanta, Georgia). The external and internal geometries were saved in a STL (stereolithography) file and were combined together using GeoMagic Studio® (GeoMagic of Research Triangle Park, North Carolina). The combined ear geometry file was converted into a NURBS surface file using GeoMagics Studio®. The NURBS surface file was saved in an IGES file format and was imported into ABAQUS CAE (based on FEM) software. Two section layers were designed in ABAQUS CAE (based on the imported ear geometry). The skin layer was designed as a membrane type (2 mm thickness) and found on the surface of the ear, where the substrate layer was designed based on the ear geometry

volume. Figure 1.5 shows the comparison of human ear picture (left), the combined STL geometry file displaying the ear cast part in red color (middle), and the NURBS surface that was created using the combined 3D geometry files (right).

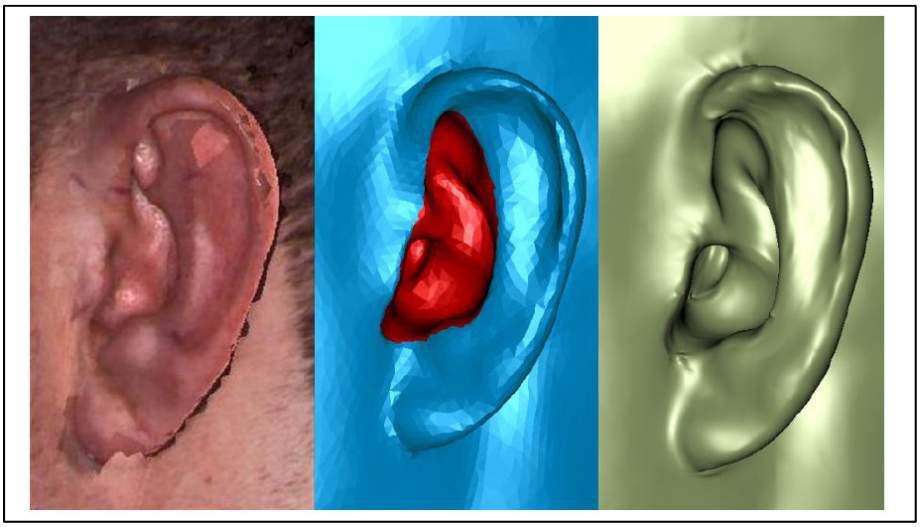

Figure 1.5 Comparison of photograph (left) STL geometry (middle) and 3D geometry files (right)
Taken from Baker et al. (2010, p. 7)

To model earplugs materials, three different earplug designs were examined. Two of the designs were constructed of a soft foam (with a hard plastic part), whereas third one was an elastic solid. The soft materials for each earplug (hard plastic parts as rigid) were examined by compressing to 20% strain (holding for 20 seconds) and were run at 0.5, 2.0 and 4.0 mm/second compression rate. The earplugs geometry were taken directly from 3D CAD drawings of the earplugs when available, whereas competitive products CAD drawings were unavailable, thus the earplugs geometry were assessed using a combination of physical measurements and 3D scanner (NextEngine) images. The 3D CAD files were saved in IGES file format to import into ABAQUS CAE software (Baker et. al, 2010).

According to the literature (Albin et. al, 2007 & Ballachanda et. al, 1995), contact pressure (SMP) plays a significant role to evaluate discomfort of earplugs. The numerical simulation was generated to measure the deformation of both the earcanal and earplugs when the

earplug was inserted completely into the earcanal. The assumption was that the earplug penetration angle and penetration depth were precisely replicated with respect to real conditions and consequently the physical details of contact between surfaces of earcanal and earplugs. The penetration depth and penetration angle were measured using taken images by the 3DMD equipment. The penetration depth and insertion angle of the earplug in earcanal were measured accurately through the relative location of the earplug to the rest of the external ear. A small foam square was considered to the earplug external end, which was provided a large enough surface to assess the penetration depth and angle. In Figure 1.6, the earplug located into earcanal and the external ear geometry are depicted.

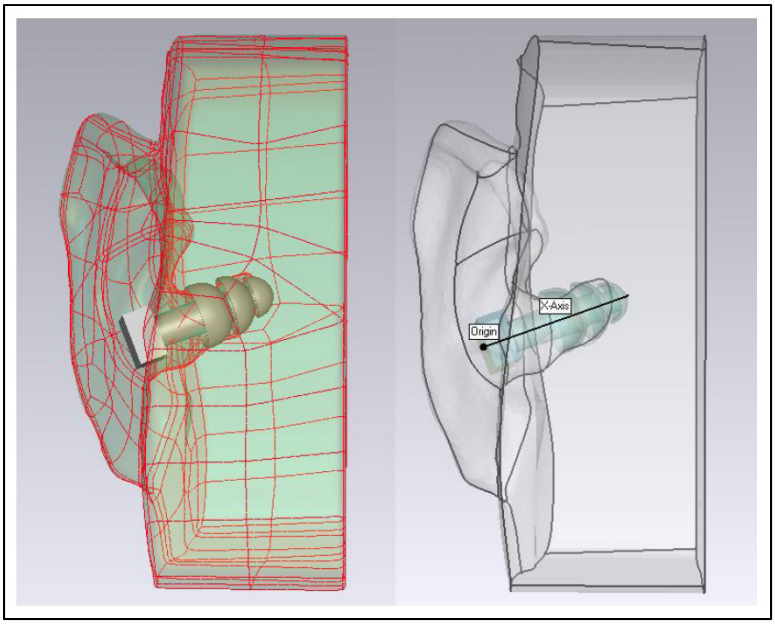

Figure 1.6 The external ear geometry with inserted earplug
Taken from Baker et al. (2010, p. 8)

The insertion depth and angle were various for each ear subject and each earplug. The x-axis of 3D ear geometry (NURBS surface) was orientated parallel to the insertion axis of earplug. The earplug origin was moved to represent the final resting position of the earplug. Transferring the earplug in the positive x-direction until earplug was contacted to the origin was corresponding to inserting the earplug into the earcanal with the correct insertion angle and depth. To simplify the boundary conditions setting, many geometry sections were

defined such as, i) the backside section of the earplug geometry was defined to constrained, ii) the surfaces on the earplugs in contact with rigid materials were adjusted as non-deformable surface, iii) during the insertion, earplug surfaces were defined to move along with the x-axis, iv) the outside surfaces of the soft earplug materials were considered as contact pairs with the outside surface of the earcanal.

The numerical simulations were divided into three continuous stages. The first stage was preparing the earplug and the external ear. Malleable earplugs need rolling between thumbs and fingers (before insertion into earcanal) to decrease their cross section area (preconditioning). This preconditioning was made easier to insert earplug into earcanal to the appropriate depth. The earplugs with soft foam were preconditioned by inducing a small displacement normal to the earplug outer surface. The preconditioning was not necessary for elastic solid earplugs (conical shape). During this stage, to increase the size of the earcanal's entrance the tragus of the external ear was pulled a bit forward (500 milliseconds duration). At the second stage, the foam material was released and the earplug was transferred along x-axis until the earplug was reached its resting place (500 milliseconds duration). At the third stage, the tragus was released and the earplug was relaxed to reach the equilibrium at the interface (500 milliseconds duration). Assumption: the friction between the earplug and the ear was in all cases were equal to zero because the friction coefficients between earplugs and earcanal skin were unknown to consider in the numerical simulation.

(Baker et. al, 2010) mentioned that some potential metrics for discomfort were considered such as average SMP, average contact force and critical contact area. Average SMP was the calculation of mean SMP for all locations, where the contact force is higher than zero. Average contact force was the calculation of the numeric mean of all contact forces (greater or less than zero). Contact force was considered in the analysis because it was related to the SMP, however contact force was not related to contact area. Critical contact area was the calculation of the total surface area under the SMP (higher than 25 kPa).

(Baker et. al, 2010) concluded that the hypothesis that discomfort has a direct relation to the contact area higher than critical pressure (25 kPa) was not correct regarding the obtained results. Moreover, the difference between earcanal sizes (small, medium and large) did not effect on measured output parameters (total contact force, average SMP and total contact area).

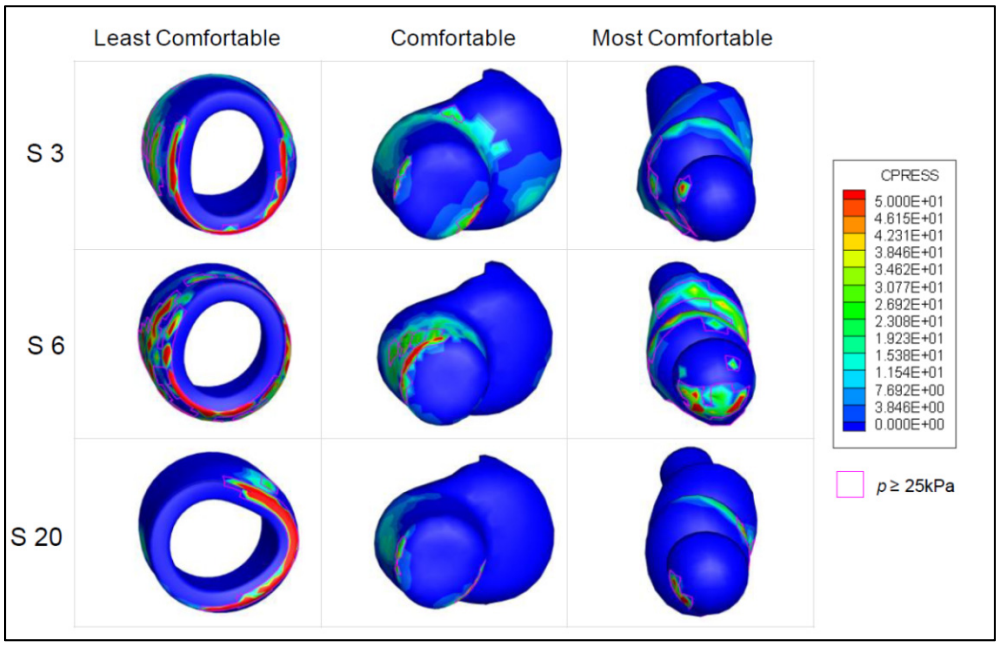

Figure 1.7 The example of contact pressure (SMP) contours for deformable part of the earplugs
Taken from Baker et al. (2010, p. 11)

In Figure 1.7, the model results is depicted, where the colors represented the differences between subjects as well as the SMP. Each row shows data from the same earcanal (S3, S6 and S20). The left column (least comfortable) shows large regions, where the SMP is concerning of 50 kPa (red color).

(Baker et. al, 2010) ceased that this preliminary numerical simulations can be used to predict the SMP as well as wearer discomfort of earplugs, however, additional works have to be

carried out to cover a wide range of earplug types. A study has to be conducted that contains these numerical simulations as an absolute measurement tool to predict the SMP.

1.7 Results of different studies for the SMP on earcanal

There are a few significant techniques to measure the SMP induced by earplug in earcanal. The following studies discuss the direct measurements of the SMP on earcanal soft tissues. (Smith et. al, 1982) published a considerable article about the measurement of expansion pressure (the SMP) of earplug exerted on the artificial earcanal walls. They used for this approach an aluminum auditory canal mounted in an Instron Universal Tester (Instron ® Corporation, Canton, Mass.). According to Figure 1.8, aluminum block (A) was divided in half (B) and a 7.54 mm diameter hole was pierced at its center along block length (C). The cylindrical hole represented the simplified external earcanal. The split aluminum block was stick to bent steel holders (D) and mounted between a load cell (E) and the crosshead (F) of the Instron Tester. The split surfaces were separated by an estimated distance (0.4 mm) or approximately 5% of the diameter of the artificial earcanal (G), because they should not touch each other (the force exerted by the touching would also be measured). Thus, the artificial earcanal was (non-cylindrical) a slightly elliptical (major-and minor-diameter of 7.9 mm and 7.5 mm) cylinder with length of the longest earplug (Figure 1.9).

Each earplug was compressed (for 15 seconds) through twirling lengthwise between the thumb and forefinger. Then, the earplug was inserted (lengthwise) and released in the artificial earcanal to relax. A measurement of force was calculated as a function of time (during five minutes). More than five minutes time was unnecessary because earplug’s relaxation was completed.

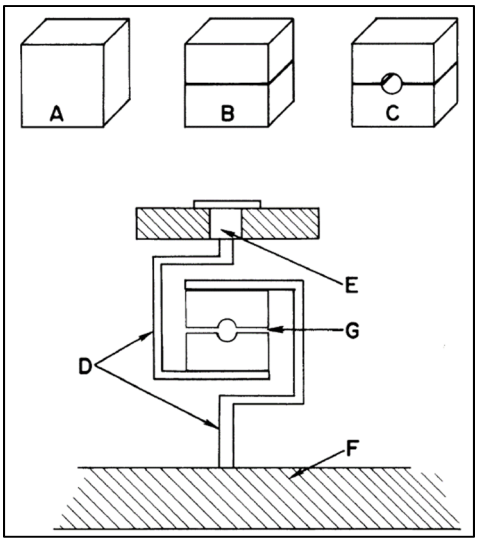

Figure 1.8 Construction of artificial earcanal

Taken from Smith et al. (1982, p. 3)

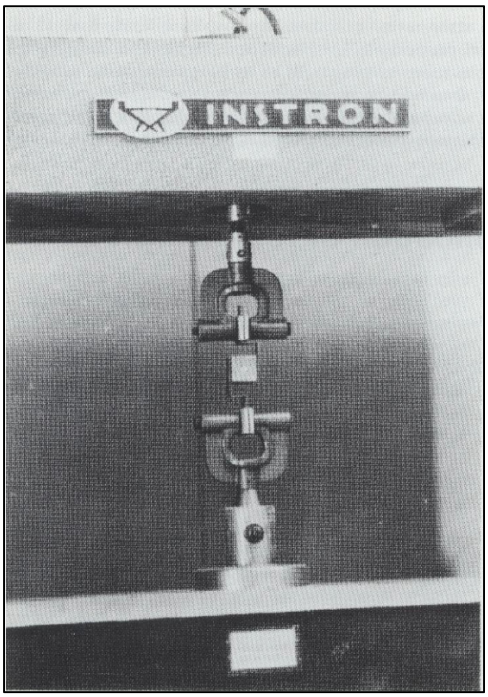

Figure 1.9 Artificial earcanal mounted in Instron® Universal Tester

Taken from Smith et al. (1982, p. 4)

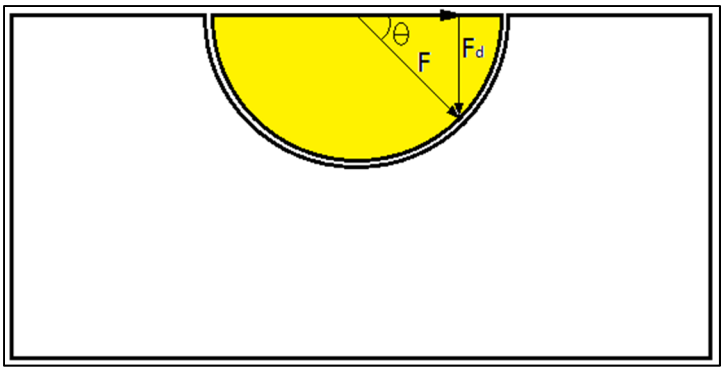

Figure 1.10 Force components for earplug expansion
in test apparatus
Taken from Smith et al. (1982, p. 3)

(Smith et. al, 1982) described a method to derive the SMP from the force measured on the Instron® Universal Tester. The following assumptions were made: the foam was induced a uniform force in all directions toward the curved surface of the cylinder (similar to a pressurized fluid inside a tube), the effects of the earplug ends was ignored. A cross section view was depicted through the constructed earcanal in the tester (see Figure 1.10).
The force exerted downward was measured by the load cell. The downward force component was calculated by

$$F_d = F\ sin\theta \tag{1.1}$$

Where, force component exerted against the load cell, force exerted against the constructed earcanal and angle shown in Figure 1.10 were represented as, F_d , F, θ, respectively. Force was defined as pressure multiplied by the area under the pressure. Thus, the total downward force was defined by

$$F = \int_0^{\pi} PrL\ sin\theta\ d\theta \tag{1.2}$$

Where, pressure generated by expansion of foam was denoted by P, the earcanal radius was defined by r , and earplug length was represented as L. The above integration was resulted in following equation, which was used to calculate the SMP,

$$F_d = -2\,PrL \tag{1.3}$$

(Smith et. al, 1982) calculated the SMP for five different types of flexible foam earplugs (E.A.R, Norton, Decidamp, Experimental and Hushler). Then, they related SMP to the acoustic attenuation of five earplugs. Although expansion force was the measurement achieved for each earplug, pressure exerted against the artificial earcanal wall (force per unit area) was expected to be the significant variable related to attenuation. The SMP was the pressure exerted by the expanding foam on the wall of the artificial earcanal. The calculated SMP and the expansion force were changeable within a single earplugs manufacturer. The SMP ranged from 4.1 kPa for the E.A.R foam to 18.8 kPa for the experimental earplug. However, in their experimental setup they measured SMP in artificial earcanal (without skin), instead of direct measurement on real subject. In Table 1.1, the summary of physical properties of five earplugs, expansion force as well as the SMP is listed.

Table 1.1 Summary* of physical properties of earplugs

Taken from Smith et al. (1982, p. 9)

Earplug Type	Diameter (mm)	Length (mm)	Weight (g)	Density (g/cm^3)	Expansion Force (N)	Expansion (Pascals)	Pressure (PSI)
E.A.R	13.79 0.11 13.58-13.94	19.04 0.43 18.20-19.40	2748 0105 2567-2889	0966 0025 0936-1019	1.033 0.151 0.764-1.161	6660 996 5159-7794	0.97
Norton	14.21 0.33 13.70-14.56	23.30 0.41 22.28-23.70	4028 0155 3700-4253	1091 0036 1036-1176	1.406 0.180 1.254-1.823	7650 1120 6651-10356	1.11
Decidamp	13.82 0.11 13.64-14.00	19.09 0.28 18.68-19.58	2818 0062 2755-2886	0984 0015 0960-1009	1.223 0.173 1.039-1.519	8223 1253 6715-10276	1.19
Experimental	14.04 0.20 13.80-14.50	19.81 0.32 19.40-20.34	7785 0208 7395-8021	2540 0074 2432-2671	2.977 0.477 2.230-3.406	18856 3565 13874-22220	2.73
Hushler	14.16 0.17 13.82-14.38	20.43 0.25 20.04-21.00	3983 0177 3864-4313	1237 0037 1168-1304	1.475 0.093 1.254-1.597	8775 1294 5491-9395	1.27

*average/standard deviation/range

1.8 Methods to calculate the SMP

For computation of SMP, some parameters have to be measured and then have to be evaluated. Those parameters are described in this section.
In order to compute SMP induced by earplugs on earcanal wall, the mechanical behaviors characterization of earplugs and earcanal (depends on the approach) are essential. A detailed explanation is in the following.

1.8.1 Mechanical behavior of earplugs

Commercial earplugs are generally made of Polyurethane (PU), Polymer vinyl chloride (PVC), Silicon and polymeric foam. The latter have porous microstructures with closed and open-air cells. In 1974, (Gardner et. al, 1974) invented a cylindrical shape earplug made of polymeric foam, whose its diameter is a bit larger than the average diameter of human earcanal. This particular earplug is produced of a *foamed plasticized polymeric* (PVC) material. This earplug contains a high concentration of plasticizer to give the earplug a reduced rate of recovery after compression. This allows the earplug to be usable for different earcanal size, because human's earcanal size and geometry are quite different regarding to gender, head size and generation. The expansion rate should be as short as possible (2 to 20 seconds) and the induced pressure have to be adequate to create a stable and fit connection with earcanal wall (at equilibrium from 2.41 to 6.89 kPa.). Three years later, (Gardner et. al, 1977) invented a conical shape earplug with similar material properties.

Soft earplugs are generally made of foam. The characterization of mechanical properties of foam earplug is a considerable challenge. (James, 2006) characterized the mechanical properties of foam earplug for different radial compression rates using a setup to measure Young's modulus and Poisson's ratio. (James, 2006) only considered an experimental setup as reference (there is no subject) and he tried to compute the sound attenuation of the earplug using FE model and thus he needed to get the earplug properties corresponding to the same compression rate as that in the experimental setup. The effects of radial compression preload on the earplugs are considered, and the resulting shear material properties of foam earplug are inserted into the finite element model (ABAQUS). This thesis develops and explores the

finite element models, which provide insight into the actual experimental response. It integrates a modern analytical material property extraction method to better characterize the 19 mm E.A.R classic foam earplug and examines the changes these new properties have on the HPD system response. The experimental system utilized to explore the EAR foam earplug validation with numerous hand calculations and simple finite element models. The EAR foam earplug material properties were determined from tests on the Dynamic Mechanical Analyzer (DMA) instrument, in the axial state. Two compression plates load the small material specimen and a known displacement is provided to the material per frequency and temperature, and a reaction force of the material is registered. The DMA test is carried out by oscillating the specimen through a prescribed displacement while sweeping through a table of frequencies and temperatures. Temperature and frequency are inversely related, testing the material at lower temperatures is equivalent to testing the material at higher frequencies. Master curves for the material's storage and loss moduli are obtained for the entire frequency range of interest using the time-temperature-superposition method. The EAR foam material was experimentally tested in the shear configuration analogous to the experimental configuration, and the material properties extracted. Radial compressive strains of 6%, 18% and 30% are explored for the EAR foam earplug.

1.8.2 Mechanical behavior of human skin tissues

The characterization of mechanical behavior of human soft tissues is difficult, because skin tissues are heterogeneous and generally demonstrate nonlinear viscoelastic (e.g. Lodge and Christensen models) and hyperelastic (e.g. Ogden and Moony-Rivlin models) mechanical behaviors (Hendriks et. al, 2003). Moreover, the in vivo characterization of mechanical behaviors of human soft tissues is a challenge, since it is not always possible to measure mechanical behavior on cadavers with all associated problems, such as safety and ethical issues. Indeed, human skin is composed of two main layers (epidermis and dermal) and a ground substance that mostly show nonlinear viscoelastic or hyperelastic behavior (Daly & Odland, 1979). New technologies can now help scientists to understand the mechanical behaviors of human skin. In this section, some appropriate technologies are mentioned for the characterization of human's skin materials.

Using ultrasound technology is another way to measure mechanical properties of the skin in vivo. A new device (echorheometer) was introduced by (Diridollou et. al, 1998). This device consists a suction system with an ultrasound scanner (mode A, mode TM and mode B) with high axial resolution 0.07 mm (Figure 1.11). The simultaneous visualization and non-invasive measurement of the deformation of skin structures were accomplished by echorheometer. The echorheometer was used to measure the behavior of skin layers (the dermis and subcutaneous fat). The results illustrated that the resistance to applied axial stress (suction) is caused by the dermis rather than the subcutaneous fat.

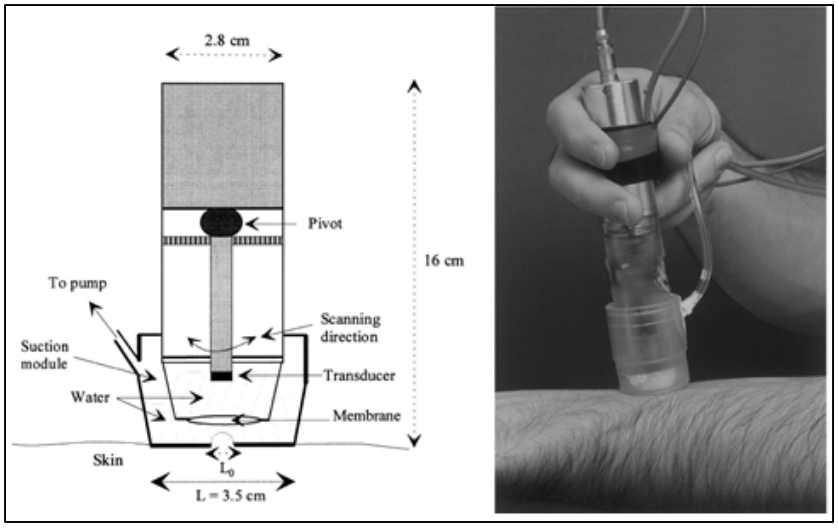

Figure 1.11 Ultrasound scanner and suction
Taken from Diridollou et al. (2001, p. 1)

The mechanical parameters of skin such as Young's modulus, the initial stress and unrestored energy ratio (non-elasticity index) were measured by a 20 MHz scan echography (Diridollou et. al, 2001). They indicated that the skin physical properties (thickness, stiffness and elasticity) alter with ageing. For instance, in vivo measurements illustrated that the Young's modulus of volar forearm was changed from 0.08 to 0.26 MPa (from 6 months to 90 years old, respectively).

The application of the finite element analysis (FEA) was proposed to the in vivo characterization of the nonlinear mechanical behavior of three human skin layers (epidermis, dermis and hypodermis). The indentation techniques was incorporated with MRI images (Tran et. al, 2007). MRI images (GE Medical System, Milwaukee, WI, USA) were processed from the left dorsal forearm of young man. Then a pre-and post-processor Patran (MSC.Software, California, USA) were used to make numerically individualized 2D model (three skin layers and muscles). To model the mechanical behavior of the three skin layers and the muscles, a Neo-Hookean (isotropic hyperelastic) slightly compressible material model were used to obtain two material parameters C_{10} and bulk modulus K. The Levenberg-Marquardt algorithm (LMA) was used to identify material model parameters. The identification obtained a range of constant values for different material properties of epidermis (C_{10}=0.12±0.06 MPa, K=5.45±1.7 kPa), dermis (C_{10}=1.11±0.09 MPa, K= 29.6±1.28 kPa) and hypodermis (C_{10}=0.42±0.05 MPa, K= 36.0±0.9 kPa). These results are used to validate the 3D numerical simulations of skin indentation tests in the master thesis. The force-displacement curves obtained from (Tran et. al, 2007) are correlated with obtained results of numerical simulation carried out in the master thesis.

The elastic mechanical properties of human skin were measured *in vivo* by using an indentation device (Skin tribometer). The skin tribometer consists of a conical steel indenter, displacement sensors and displacement tables (X, Z). A schematic of skin tribometer device is depicted in Figure 1.12. The indentation tests are performed in controlled displacement mode, where displacement in Z-direction was obtained by using National Instrument displacement table and displacement was controlled by a sensor. The maximum displacement during the loading-unloading cycle can reach about 15 mm. The indentation tests were realised for a constant speed (400 µm/s). In order to simplify the study, the skin is considered as an elastic soft thin layer on a rigid substrate. Three different analytical mechanical (Bec/Tonck) models were used to evaluate the effect of subcutaneous layers on the measurements and to extract the skin elastic properties from the global mechanical properties. To estimate the skin Young's modulus, it was necessary to consider the effect of

the subcutaneous layers. All models gave an average value of the inner forearm skin Young's moduli between 4.5 kPa and 8 kPa (Pailler-Mattei et. al, 2008).

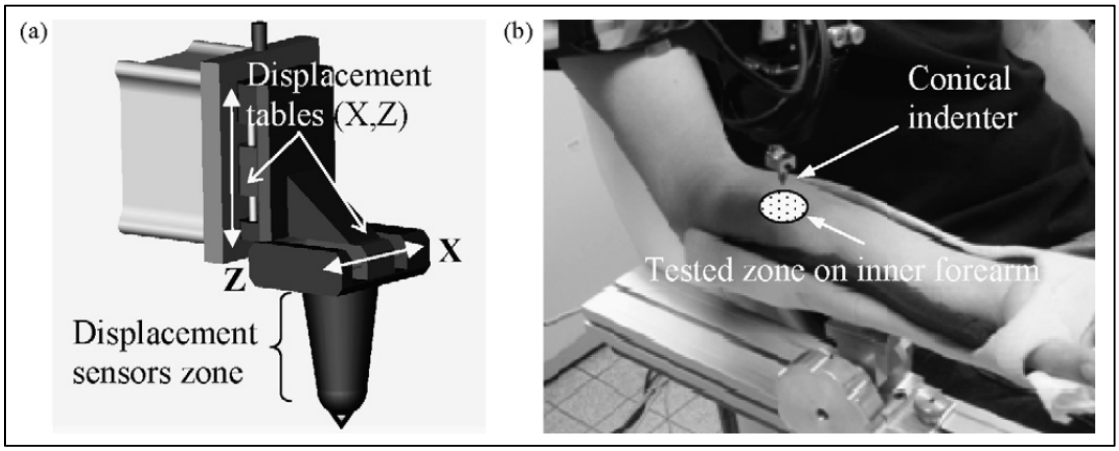

Figure 1.12 Skin tribometer device: schematic of indentation device (a)
indentation system and positioning (b)
Taken from Pailler-Mattei et al. (2008, p. 2)

Few details are provided in the publications concerning the measurement and calculation of the SMP applied by earplugs on the walls of the earcanal (Rickie Davis, 2008 & Baker et. al, 2010). In fact, most of the works in the field has been conducted for the military or private research laboratories. Some patents mention SMP measurement devices but the scientific content is generally not rich (Gardner et. al, 1974, Gardner et. al, 1977 & Gardner et. al, 1992). The first important study on the SMP is from (Smith et. al, 1982).

Since the materials of human earcanal are highly nonlinear and viscoelastic (Daly & Odland, 1979), then numerical simulation of earcanal soft tissues is an enormous challenge. In order to facilitate the numerical simulation and modeling of earcanal soft tissues (i.e. skin), using numerical simulation tools, whose working based on finite element method (FEM) is greatly helpful and reliable. FE method does not solve the problem of determining the behavioral laws of soft tissues and earplugs. Indeed, FE method is used to validate the experimental data obtained from test setups (Qi & Liu, 2007). Human skin consists three main layers, which show nonlinear viscoelastic and hyperelastic mechanical behaviors under the SMP (Tran et.

al, 2007& Qi and Liu, 2007). A large deformation of earcanal skin layers is induced upon insertion of earplug (depends on the types of earplug) inside earcanal. For instance, a large deformation occurs when a compressed foam earplug is inserted in earcanal and relaxes. This deformation induces large strain on skin of earcanal wall (Benacchio, 2018).

1.9 Assessment of literature review and originalities of the proposed research work

By help of the literature review the following aspect are concluded about the numerical simulation of SMP:
In the literature, there are few publications corresponding to numerical simulation of the SMP on earcanal. Whereas, numerical tools based on FEM could be used to predict the SMP on earcanal, they are not fully validated yet. The originality of the project here is the evaluation of simplified experimental tester data using corresponding numerical model.

As mentioned before, limited number of research has been performed to evaluate the SMP exerted by an earplug on human's earcanal wall. The characterization of earcanal skin and substrate layers will be assessed according to work of (Tran et. al, 2007).

Accordingly, there is no accessible test bench for assessing the SMP in this part of the body. The development of such test bench is a challenge given the complicated geometry of the earcanal as well as the available sensor technologies. A few attempts were made to estimate the SMP by numerical computations, but models are limited, particularly regarding the simple behavior laws and physical parameters used. Moreover, no model validation was carried out.

In the next chapter, the research problems and its main and specific objectives will be explained in more detail, which are necessary for the reader to understand the scope of dissertation.

CHAPTER 2

RESEARCH PROBLEMS AND OBJECTIVES

In this chapter, research problems relative to prediction of the static mechanical pressure (SMP) exerted by a foam earplug inserted into an earcanal are outlined. At the end of this chapter, related research main objective and specific objectives are explained.

2.1 Problems of numerical simulation for the computation of the SMP

The earcanal is an organ, which consisting of various components such as skin, cartilage, soft tissues and bone. Each separate component has different material properties and the combination of those various components has a significant influence on the evaluation of the SMP on earcanal. The complexity of the geometry of earcanal leads to difficulties for the prediction of the SMP. Moreover, the mechanical properties of earplugs have effects on the evaluation of the SMP.

Computation of the SMP by using numerical simulation tools requires modeling of the solid geometries of earcanal and earplugs with regular and high quality number of finite elements. Because both solid geometries (earcanal and earplug) have small sizes and earcanal has complex geometry. High quality number of finite elements causes increase of precision in numerical simulation results. Moreover, the SMP values are low, between 6.68 kPa and 18.82 kPa (Smith et. al, 1982), which requires high number of finite elements. The increasing number of finite elements (mesh refinement) will improve the quality and accuracy of numerical simulation, which is time consuming.

2.1.1 Problems of numerical simulation of foam earplug deformation

A considerable problem will be computation of earplug deformation during preconditioning (radial compression) (Gardner et. al, 1974 & Gardner et. al, 1977) and during insertion into

earcanal. For instance, 3M classic foam earplug requires preconditioning before insertion inside earcanal. The preconditioning causes 60% reduction of earplug's diameter (Gardner et. al, 1974), which is a large strain. Numerical simulation of such a large strain is difficult to achieve because 3M classic foam earplug consists of open and closed cells in microstructure and there are some mathematical formulation problems for material modeling.

2.1.2 Problems of numerical simulation of earcanal soft tissues deformation

The computation of skin's large strain is a difficult challenge for numerical simulation, because earcanal skin consists of layers with different mechanical properties and the simulation of these layers above each other requires high quality and a high number of finite elements, because high number of finite elements increases precision of obtained results. Obviously, high number of finite elements requires high processing computers (HPC) for exact numerical simulation as well as convergence of simulation. FE-modeling software LS-Dyna (Livermore Software Technology Corporation) can be used to simulate numerically skin's large strain.

2.1.3 Contact problems in simulation of two deformable solids

The deformation study of two solids, which touch each other at several points, is defined as contact mechanics (Johnson et. al, 1985). In contact mechanics, the normal stresses act perpendicular to the surfaces of contacting bodies, while frictional stresses act tangentially between the bodies' surfaces. The ability to model interaction between two solid bodies (contact mechanics) with consideration of friction, thermal, electric or other forms of exchange is critical for numerical simulation tools (Bhashyam, 2002). The accuracy and robustness in simulations of contact mechanics can be affected by the element type (one of the most important choices) used to discretize the geometries of deformable bodies (Maas and Ellis, 2016). FE modeling of contact between two deformable solids (earcanal and earplugs) has some difficulties such as nonlinear problem, where nonlinear problem requires slow change of boundary conditions. Two examples of nonlinear problem are infinite looping and convergence to the wrong solution. Another contact problem in FE modeling is penetration of master body (earplug) to slave body (earcanal). There are different types of

penetration in FE modeling such as volume intersection, surface in volume, segment in volume, nodes in volume and nodes to surface (Yastrebov et. al, 2010).

2.1.4 Problem of having access to experimental values of the SMP

To validate results of the SMP obtained by numerical simulation, having access to experimental values of SMP is necessary. To measure the SMP values inside earcanal, flexible pressure sensor with high precision is required. As mentioned before, the earcanal has an average diameter equal to 7.5 mm, which is very small. The available flexible pressure sensors are too bulky, and cannot be inserted inside earcanal.

2.2 Research objectives

The main objective of this research project is to design virtual testers to predict the static mechanical pressure (SMP) exerted by a foam earplug inserted into a simplified cylindrical earcanal. More specifically, numerical models and simulation of testers of increasing complexity will be developed for respectively computing the SMP induced by a roll-down cylindrical foam earplug in an earcanal.

Accordingly, the specific objectives of this project are to compute the SMP using finite element models (FEM) with two levels of complexity:
1) a FEM that simulates the insertion of a roll-down cylindrical foam earplug in a simplified rigid earcanal of cylindrical shape without skin layer.
2) a FEM that simulates the insertion of a roll-down cylindrical foam earplug in an earcanal of cylindrical shape that includes the surrounding soft tissue (skin).

In the next chapter, the research methods used to achieve the specific objectives are presented.

CHAPTER 3

RESEARCH METHODS

A roll-down cylindrical foam earplug was chosen in this master thesis, because these types of earplug are more common to wear with respect to other types. To simulate the insertion of a roll-down cylindrical foam earplug in a simplified cylindrical earcanal and compute the SMP, four main steps were followed:

1) define the material law and mechanical properties of a roll-down cylindrical foam earplug from experiments performed in house;

2) define the material law and mechanical properties of the human skin FEM from literature data;

3) create a FEM of the foam earplug-rigid earcanal interaction, use the model to compute the SMP and validate the model using experiments performed in similar conditions (objective 1);

4) add a skin layer to the earcanal and recompute the SMP (objective 2).

3.1 Material law and mechanical properties of roll-down cylindrical foam earplug

In order to define the material law and mechanical properties of the foam earplug, a finite element simulation that replicates compression tests of a roll-down cylindrical foam earplug in both axial and transverse directions was performed.

3.1.1 Mechanical characterization of a roll-down cylindrical foam earplug behavior

To characterize the mechanical behavior of a foam earplug, a servo-hydraulic mechanical testing machine (MTS Mini Bionix 850, MTS Systems & Corporation, Eden Prairie, USA) was used to compress 8 foam earplugs in both axial (Figure 3.1) and transvers directions (Figure 3.2).

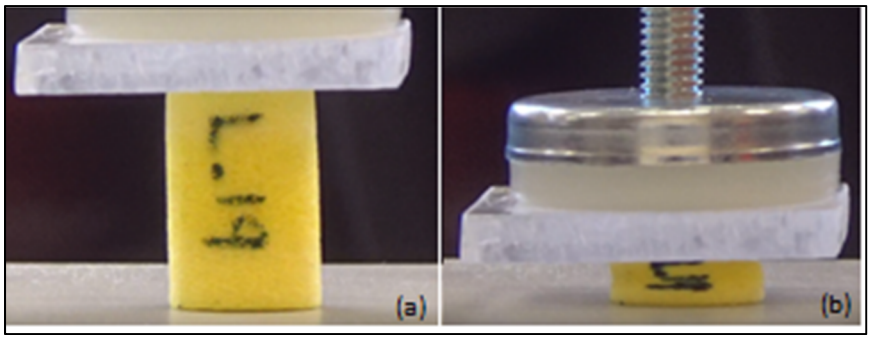

Figure 3.1 Axial compression test setup (a) before compression
(b) after compression

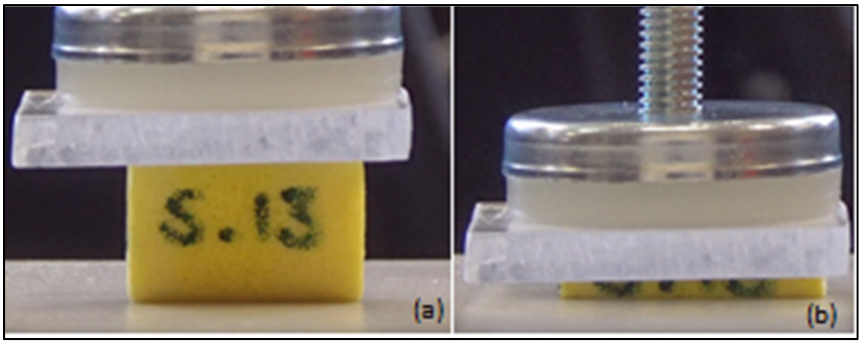

Figure 3.2 Transverse compression test setup
(a) before compression (b) after compression

All tested roll-down cylindrical foam earplugs were 3M classic E.A.R made of PVC foam (Figure 3.3). Earplugs had an average diameter of 13 mm and a length of 20 mm. The compression rate was 0.1 mm/s in both compression tests and the acquisition frequency was equal to 10 Hz. In both axial and transverse directions, earplugs were compressed up to 80% of their total length and diameter, respectively. The experiment was performed by Elisabeth Laroche eng., MASc, a research assistant at ETS. Force-displacement curves were extracted for each test and used to build an average force-displacement experimental curve that represents the mechanical behavior of the earplug.

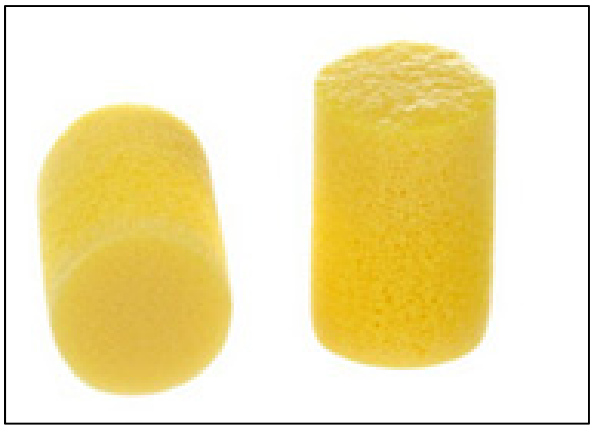

Figure 3.3 E.A.R 3M classic FOAM

3.1.2 Numerical simulation of the foam earplug axial compression test

A finite element model of the foam earplug was built and used to drive the material law and properties of the foam earplug, which best replicates the results of the axial compression test previously described.

3.1.2.1 Geometry, meshing, loading and boundary conditions

The geometry of a 13 mm diameter cylinder of 20 mm long was first created and vertically positioned to reproduce the earplug. The cylinder was meshed using cubic solid elements with a characteristic length of 0.5 mm (Figure 3.4a). Two plates meshed with linear brick elements of 2.0 mm were added on above and below the cylinder to mimic the top and base plates of the MTS machine (Figure 3.4b). Both plates were defined as rigid bodies. Meshing size was defined using a convergence study in order to have reasonable calculation time without compromising result accuracy (see Appendix AI). The bottom plate was fixed in X, Y and Z-directions.

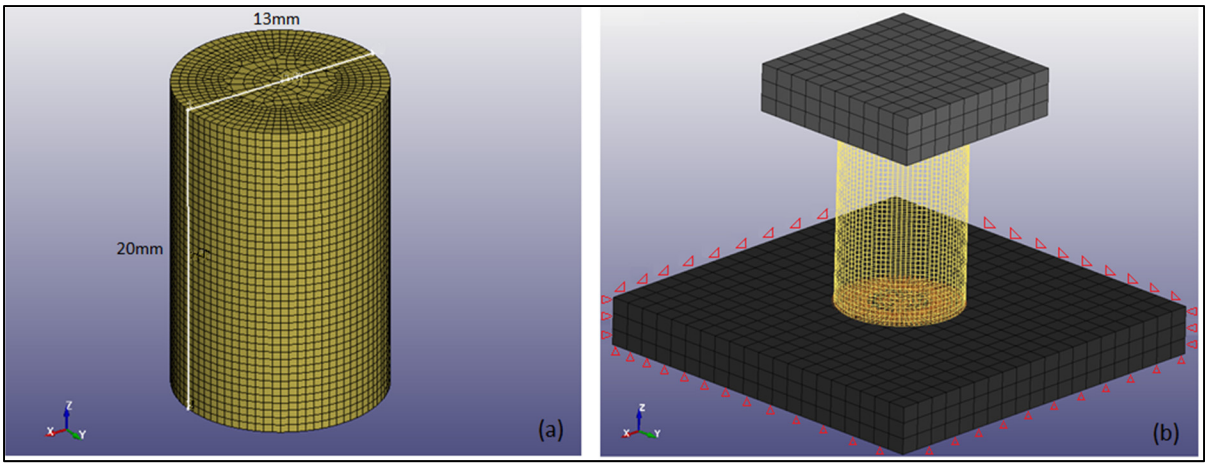

Figure 3.4 Dimension of the axial foam earplug (a) and boundary conditions of the FE simulation (b)

The top plate was free to move in the Z-direction only. The axial load was applied through the axial movement of the top plate at a constant rate of 0.1 mm/s, up to 16 mm compression (80% of the total length of the earplug), as performed during the experiment. The contact surface between the earplug and the two rigid plates was frictionless.

3.1.2.2 Material model

To simulate the roll-down cylindrical foam earplug mechanical behavior, the material model named *MAT_HILL_FOAM was selected from list of material models available in LS-Dyna. This material model simulates the non-linear hyperelastic (highly compressible) behavior of the foam earplug and is based on a strain energy function defined by (Hill et al, 1979) and (Storakers et al, 1986). The viscoelastic behavior of the earplug was neglected. The strain energy function proposed by (Hill et al, 1979) is explained by the following equation:

$$W = \sum_{j=1}^{m} \frac{C_j}{b_j}\left[\lambda_1^{b_j} + \lambda_2^{b_j} + \lambda_3^{b_j} + \frac{1}{n}(J^{-nb_j} - 1)\right] \quad (3.1)$$

In the abovementioned function, $J = \lambda_1\lambda_2\lambda_3$ defines the ratio from deformed state to non-deformed state of foam earplug. The material constants are C_j , b_j and n.

The main Cauchy stress can be defined by:

$$t_i = \sum_{j=1}^{m} \frac{C_j}{J}\left[\lambda_1^{b_j} - J^{-nb_j}\right] \quad i = 1,2,3 \tag{3.2}$$

The shear modulus can be obtained by:

$$\mu = \frac{1}{2}\sum_{j=1}^{m} C_j\, b_j \tag{3.3}$$

Continuously, the bulk modulus (K) can be defined by:

$$K = 2\mu\left(n + \frac{1}{3}\right) \tag{3.4}$$

The required parameters for this hyperelastic material model are the density ρ_{Foam}, the bulk modulus K_{Foam} and material constants b_{Foam} and n_{Foam}. The density of earplug is calculated by using following equation:

$$\rho = \frac{Weight}{Volume} \Rightarrow \tag{3.5}$$

$$\frac{0.308\ gram}{2903.872\ mm^3} = 1.06065 \times 10^{-4}\ \frac{gram}{mm^3}$$

The values of other parameters are:

$$K_{Foam} = 0.131\ MPa$$
$$b_{Foam} = 13.15$$
$$n_{Foam} = 0.022$$

These aforementioned material parameters were obtained by running FEM of compression tests exactly similar to experimental tests. In more details, an inverse method is used to drive material parameters. These parameters were significant in works of (Hill et al, 1979) and

(Storakers et al, 1986). Thus, they were chosen from their work at the beginning. They were slightly changed to fit experimental test data like a trial and error method. The force-displacement curves of FEM and experimental tests were compared until both curves matched. Using an optimization method was also possible to match two curves. The compared curves were resulted a very good match between FEM and experiments.

3.1.3 Numerical simulation of foam earplug transverse compression test

The numerical simulation of the transverse compression test of the foam earplug is similar to the simulation of the axial compression test. The only different was the orientation of the earplug, which was rotated by 90 degrees around the Y-direction.

3.1.3.1 Geometry, meshing, loading and boundary conditions

As in the simulation of the axial compression test, the medium size foam earplug had a length of 20 mm and a 13 mm diameter was discretized by cubic solid element with a characteristic length of 0.5 mm (Figure 3.5a). The top and bottom rigid plates were discretized by cubic solid element with a characteristic length of 2.0 mm. The bottom plate was fixed in X,Y and Z-direction (Figure 3.5b).

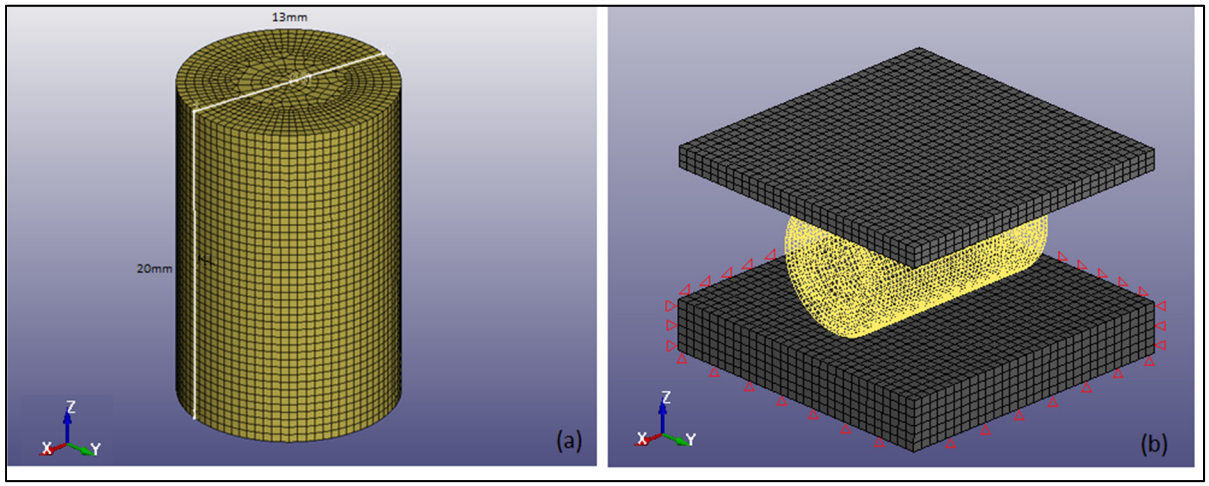

Figure 3.5 Dimension of the transverse foam earplug (a) and boundary conditions of the FE simulation (b)

The top plate was free to move in the Z-direction (vertical) only. The vertical movement of the top plate had a rate of 0.1 mm per second, as in the experiment. The contact surface between the earplug and two plates was frictionless.

3.1.3.2 Material model

The material model and parameters of the earplug for the simulation of the transverse compression test are the same as in the axial compression test simulation. Accordingly, the foam of the earplug was considered as an isotropic material. Similar to simulation of axial compression test, an inverse method is used to drive material parameters. The material parameters were used from works of (Hill et al, 1979) and (Storakers et al, 1986). They were slightly changed to fit experimental test data. In more details, a numerical simulation (LS-Dyna) software was run and then used to ensure that the material properties obtained previously for the earplug model were also providing good results in transverse compression. This was done by comparing the force-displacement curve obtained numerically with those obtained experimentally during transverse compression.

3.2 Material law and mechanical properties of human skin

Due to the complex composition (three layers) of human skin and difficulties of *in vivo* tests, the characterization of mechanical properties of human skin is a challenge. Some methods are mentioned in the literatures such as indentation tests (Delalleau et. al, 2006 & Tran et. al, 2007), suction tests (Diridollou et. al, 1998) and twist tests (Agache et. al, 1980). In this work, the mechanical properties of human forearm skin were defined using the work of (Tran et. al, 2007). To produce the hyperelastic material behavioral law of the three skin and muscle layers, a nonlinear Neo-Hookean slightly compressible material model (homogeneous and isotropic) was used. The *MAT_HYPERELASTIC_RUBBER was thus selected in the LS-Dyna software and a simulation that mimic the experiment of Tran et. al, (2007) was

defined to verify that their material parameters, defined using 2D finite element model, were suited for our 3D model.

3.2.1 Numerical simulation of the skin indentation test performed by Tran et. al (2007)

3.2.1.1 Geometry, meshing, loading and boundary conditions

The numerical simulation of the indentation test performed by Tran et. al, (2007) was conducted using LS-Dyna software. In Tran et. al, (2007) work, a cylindrical rigid indenter (radius =6.22 mm) was used to quasi-statically indent the three skin layers, namely the epidermis, dermis, hypodermis and the muscle layer of the forearm to derive the hyperelastic material model and parameters that best describe their mechanical behavior (Figure 3.6).

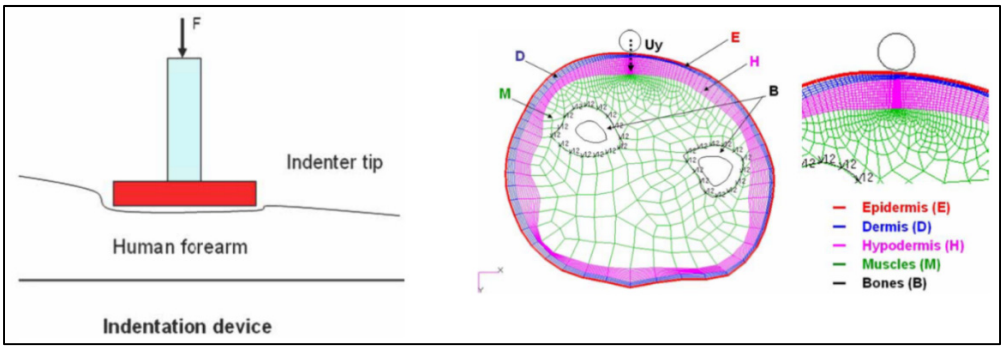

Figure 3.6 Setup of the skin indentation test

Taken from Tran et al. (2007, p. 2)

The geometries of indenter, skin and substrate layers (epidermis, dermis, hypodermis and muscle) as well as their dimensions are depicted in Figure 3.7. The length of the cylindrical indenter is equal to 60 mm, with a 6.22 mm radius. The dimension (width × length × height) of the epidermis layer is 60×120×2 mm^3. The dimension of the dermis layer is equal to 60×120×2 mm^3, the dimension of the hypodermis is equal to 60×60×10 mm^3 and the dimension of the muscle layer is 60×120×50 mm^3. The indenter is a cylindrical rigid body, which was discretized by cubic solid elements with 1.2 mm element size (Figure 3.7). The indenter was allowed to move along the negative Z-direction and to indent the skin by 7.5

mm. The skin layer and the substrate layers were discretized by cubic solid elements of 4 mm length. A mesh refinement procedure was applied to discretize the skin elements under the indenter to a finer size. The mesh refinement has increased the accuracy of the numerical simulation, but the computation time was doubled. In order to eliminate slippage between the skin and the substrate layers (four layers) at their interfaces, the elements of the epidermis and the dermis layers were merged to the hypodermis and muscle layers. The bottom surface of the substrate layer (muscle) was fixed in all directions, while the rest of the model was free to deform. Moreover, the area under the indenter (top of the epidermis) was the zone where stress and strains were analyzed. The nodes of this zone are highlighted in red in Figure 3.7.

The contact condition between the indenter surface and the epidermis was modeled using a node -to-surface contact in LS-Dyna. Ballpoint algorithm was used for contact detection. The penalty method was used to manage the contact interaction because this method provides no convergence problem and much more accurate results than mortar method.

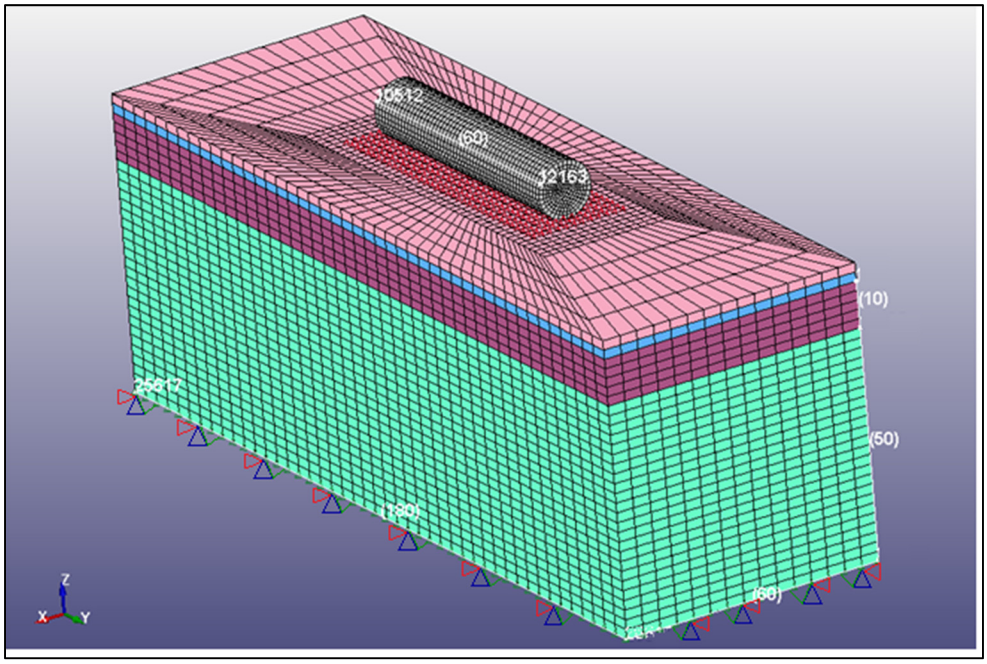

Figure 3.7 Boundary conditions and mesh structures of indenter skin and substrate layers in LS-Dyna (fixed bottom surface)

3.2.1.2 Material model

A Neo-Hookean nonlinear hyperelastic material behavioral law was used to model the mechanical behavior of the skin and substrate layers, which are considered homogeneous and isotropic (Tran et. al, 2007). The Neo-Hookean material law is defined by the following strain energy equation:

$$W = C_{10}(I_1 - 3) + 0.5\,K(J-1)^2 \tag{3.6}$$

where the first invariant of the strain tensor is denoted by I_1, the Neo-Hookean parameter is defined by C_{10}, the bulk modulus is denoted by K and the volumetric ratio is defined by J. To simulate skin layers indentation test, the material properties C_{10} and K defined by Tran et. al, (2007) for the skin layers (epidermis, dermis, hypodermis and muscle) were inserted into LS-Dyna software. Those material properties are:

$$C_{10Epidermis} = 0.12\ MPa$$
$$C_{10Dermis} = 1.11\ MPa$$
$$C_{10Hypodermis} = 0.42\ KPa$$
$$C_{10Muscle} = 3.64\ KPa$$

$$K_{Epidermis} = 5.45\ MPa$$
$$K_{Dermis} = 29.6\ MPa$$
$$K_{Hypodermis} = 36.0\ KPa$$
$$K_{Muscle} = 143.8\ KPa$$

Those Neo-Hookean material properties were defined in the material model *MAT_HYPERELASTIC_RUBBER available on LS-Dyna. The FE model was improved to assess material properties of skin layers.

Due to the low value of the bulk modulus and the Neo-Hookean parameter (K and C_{10}, respectively) for the skin and the substrate layers (particularly for the hypodermis), dynamic relaxation algorithm as well as decreasing rate of indenter movement were applied to obtain appropriate results.

3.3 Finite element modeling and validation of the interaction between a roll-down foam earplug and a simplified rigid cylindrical earcanal to compute the SMP (objective 1)

The numerical simulation of the static mechanical pressure (SMP) in a simplified cylindrical rigid cylindrical earcanal was carried out by first compressing radially a foam earplug of a larger diameter than the earcanal (to simulate the roll-down process), then by inserting the initially compressed earplug inside the cylindrical earcanal and finally, by releasing the compression to let the earplug expand until equilibrium is reached.

A simplification of the geometry of the earcanal is proposed in this work since the earcanal geometry is very complex. For the first objective, a cylindrical pipe with circular cross-section and rigid walls made of steel was used to mimic a simplified human earcanal. This first simulation is an important simplification compared to the work of (Baker et. al, 2010), but the idea is to provide a first simple but validated tool to estimate the SMP. In addition, the first simulation is dependent on: (1) the geometry of the non-deformed foam earplug, and (2) the mechanical properties of the foam earplug, which were both defined in a previous section.

3.3.1 Geometry and meshing

The inner and outer diameters of the pipe representing the earcanal were equal to 7.5 mm (similar to the average of a human earcanal) and 12.68 mm, respectively (Figure 3.8a). The pipe was 20 mm long. The finite element model of the earcanal was developed by meshing the pipe using solid 8-nodes brick elements with a characteristic length of 0.5 mm (Figure 3.9a). To model the earplug, a volume of cylindrical shape (3M classic roll-down foam

earplug; Figure 3.8b) of 13 mm diameter and 20 mm long was meshed using the parameters described in section 3.1 (Figure 3.9b).

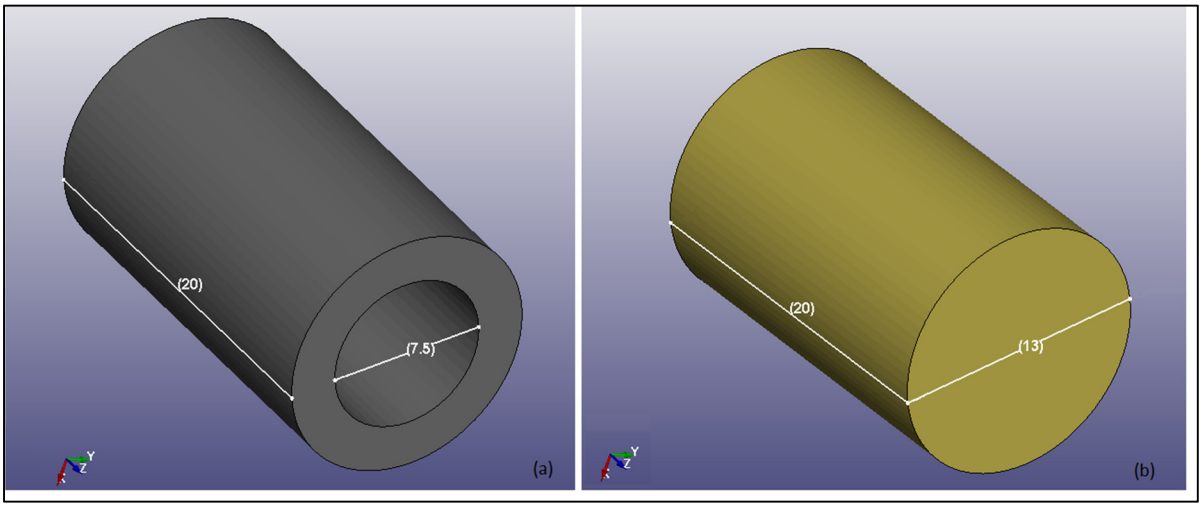

Figure 3.8 Geometries and dimension of the cylindrical earcanal (a) and foam earplug (b)

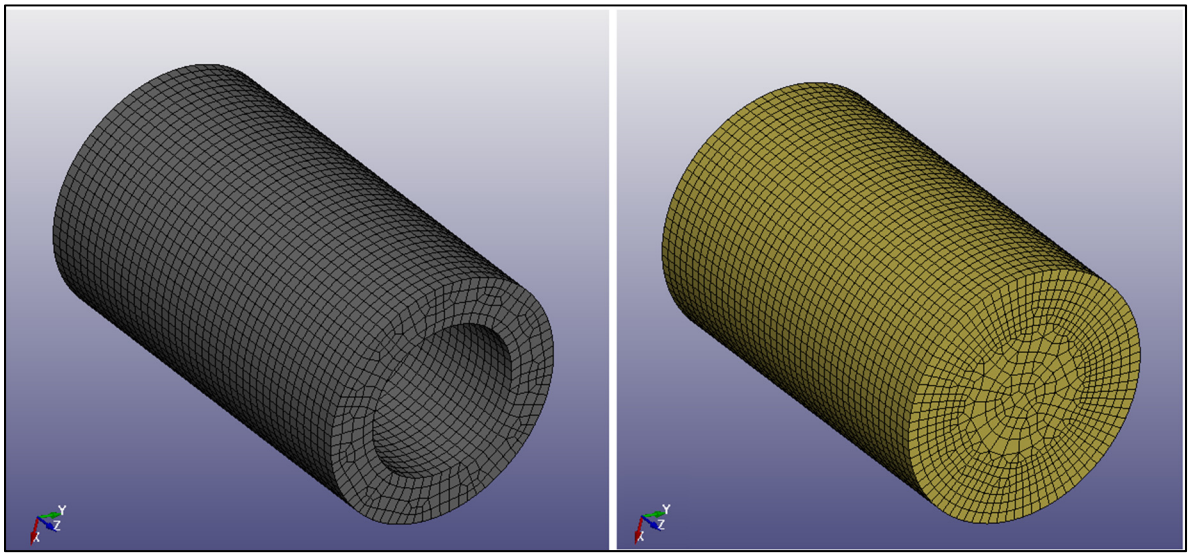

Figure 3.9 Meshed structure representing the cylindrical earcanal (a) and earplug (b)

3.3.2 Loading and boundary conditions

All nodes of the cylindrical earcanal were rigidly linked and fixed in the three directions (X, Y and Z-direction). The simulation of the SMP was carried out in three stages. Firstly, a

small radial (normal to the surface) displacement at the surface of the earplug was applied to produce the compression (roll-down) and pre-stressed condition of the earplug preceding its insertion. To create radial displacements on earplug surface nodes, providing a local coordinate system at each node was required. An example of a local coordinate system is shown in Figure3.10a. The Z-direction of the local coordinate system is along the cylindrical earcanal center axis, while the X-direction is normal to the surface and points toward the center of the earplug (radial compression direction). The Y-direction is the cross-product of the X-and Z-direction. In addition, for each surface node, a specific vector was created (nodal vector). The nodal vector is in the negative X-direction. The nodal vectors and displacement directions are depicted for each surface node in the Figure 3.10b. The diameter of the foam earplug after compression was equal to 5.44 mm, which represents a 60 percent reduction.

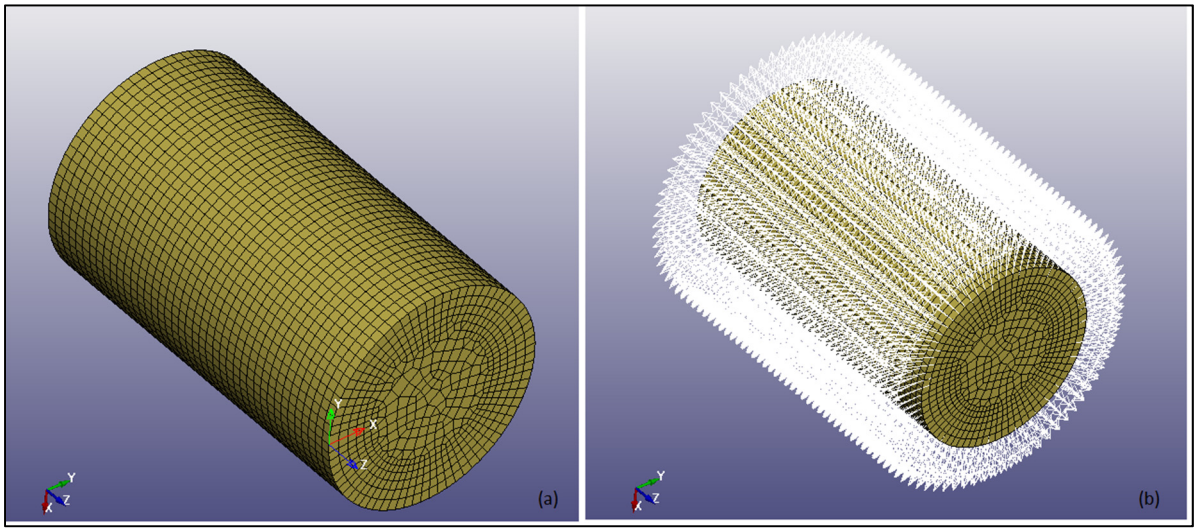

Figure 3.10 Typical local coordinate system (a) and nodal vectors for earplug surface nodes (b)

The earplug was moved along the cylindrical earcanal axis to reproduce an earplug insertion without contact with the earcanal wall until it was completely inserted in the channel. Finally, the normal displacement at the surface of the earplug was removed, allowing the earplug material to expand, lean against the walls of the rigid earcanal up to equilibrium and calculate the SMP at the interface between the earplug and the earcanal.

The yellow triangles in Figure 3.11 represent the nodes at the inner surface of the rigid cylinder in contact with the earplug after expansion. The inner surface area is the scope of the SMP prediction. The red arrow shows the direction of the earplug insertion, along the axis of the rigid cylinder.

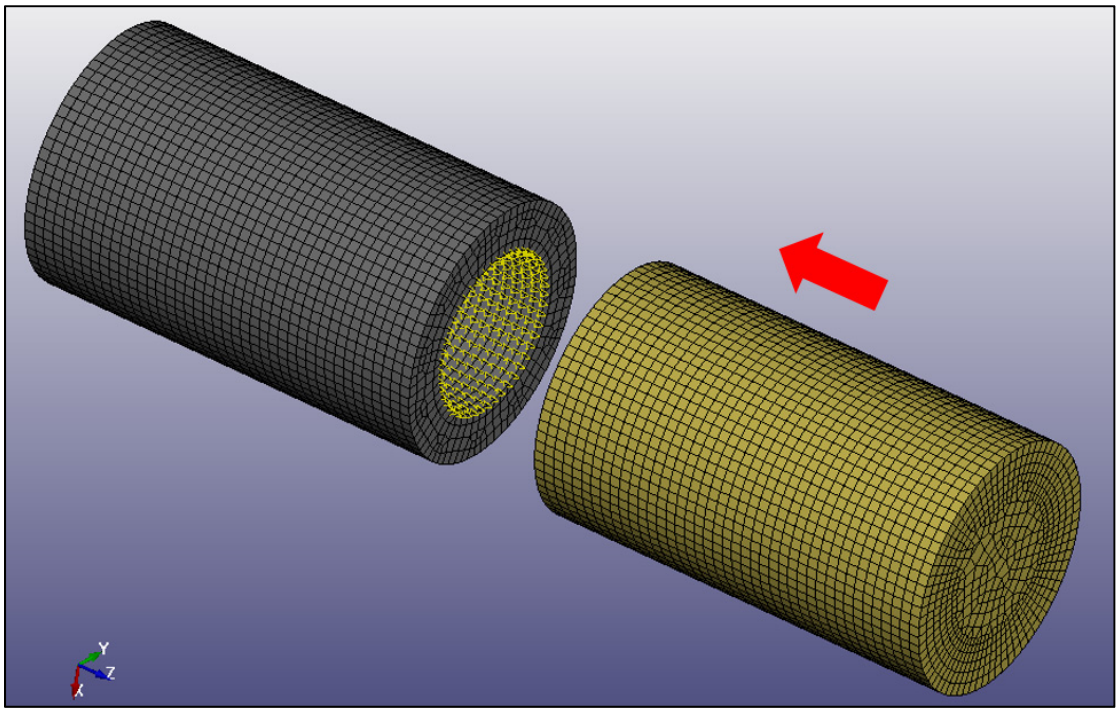

Figure 3.11 Nodes at the inner surface of the rigid cylinder in contact with the earplug after expansion

3.3.3 Contact conditions

A frictionless contact interface was defined between the earplug and the earcanal wall. The contact condition between the inner surface of the cylindrical earcanal and the earplug plays a significant role to compute SMP accurately. The penalty method was used to simulate contact. A penalty factor of 0.1 was applied and a ballpoint algorithm was used to search connection between nodes at the interface. The cylindrical earcanal was considered as the slave part, while the earplug was considered as the master part. The cylindrical earcanal was defined as a rigid body.

3.3.4 Validation of the model

The computed SMP values were verified by comparing the values obtained numerically to the results of the experimental tests. According to work of (Smith et. al, 1982), an experimental test was performed by Elisabeth Laroche eng., a research assistant at ETS. Through this test procedure the expansion of foam earplugs with different diameters were measured. The experimental device (MTS Mini Bionix 850, MTS Systems & Corporation, Eden Prairie, USA) was used to compress 8 foam earplugs in radial direction (Figure 3.12).

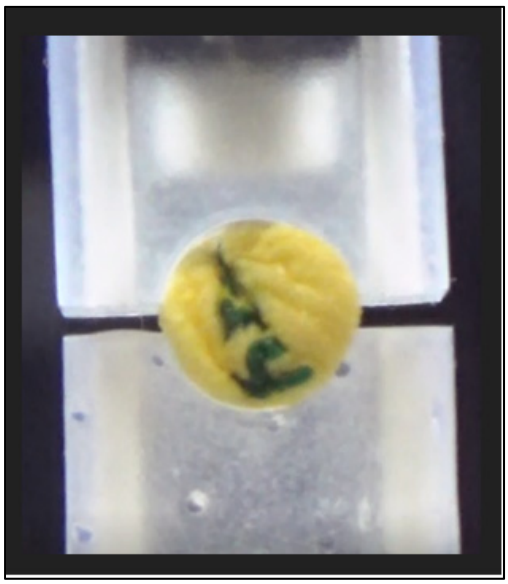

Figure 3.12 Radial compression and expansion test setup of the roll-down foam earplug

All tested foam earplugs were 3M classic E.A.R made of PVC foam. Earplugs had an average diameter of 13 mm and a length of 20 mm. A mold was manufactured to measure force induced by foam earplug at the interface between foam earplug and cylindrical mold after radial compression (80% diameter) of foam earplug and then insertion inside mold. In fact, the foam earplug was radially compressed and inserted inside hole of mold and then was relaxed for 300 seconds. The bottom part of mold was fixed while top part was moved in Z-direction. The expansion of foam earplug was caused movement of top part, gradually.

Through this movement, the force value was measured at the interface of foam earplug and inner surface of mold hole. Force-time curves were extracted from experimental tests.

3.4 Finite element modeling of the interaction between a roll-down foam earplug and a simplified cylindrical earcanal with a skin layer to compute the SMP without validation (objective 2)

In the second objective, a thin skin layer with a thickness of 0.5 mm was added inside the cylindrical rigid earcanal of the FEM of objective 1 to mimic the skin of the human earcanal (Viallet, 2014). There was no validation of the numerical model in this section. The thin skin layer was modeled and merged to a cylindrical rigid earcanal with 8.5 mm diameter. Thus, the canal with the added skin layer had the same final diameter (7.5 mm) as the rigid canal described in objective 1 (Figure 3.13a). The layer was meshed using the same elements as the rigid earcanal (Figure 3.13b). The mechanical properties of the skin layer were the one described for the epidermis in section 3.2.1.2. The epidermis layer was selected because this layer had the highest bulk modulus with respect to other skin layers. High bulk modulus prevented penetration of the foam earplug's elements to the skin layer's elements. The penetration of elements of two semi-solids caused convergence error in numerical simulation.

The geometry, the mesh and the material properties of the earplug, as well as the loading and boundary conditions were the same as the one used for objective 1 (Figure 3.13b and Figure 3.14b).

The yellow triangles in Figure 3.15 represent the nodes at the inner surface of the skin layer inside the rigid cylinder in contact with the earplug after expansion. The inner surface area is the scope of the SMP prediction. The red arrow shows the direction of the earplug insertion, along the axis of the rigid cylinder.

A frictionless contact interface was defined between the skin and the earplug using the penalty method. However, in this numerical simulation, both earplug and skin layer were deformable bodies which increase the complexity of the numerical simulation. The earplug was considered as master part, whereas the skin layer was considered as slave part. The

ballpoint algorithm was used to search contact at the interface, when the earplug touches the skin layer.

The simulation of the SMP was carried out using the same three stages described in objective 1. This second simulation is closer to the works of (Baker et. al, 2010). Although the geometry of the earcanal is still simplified, this simulation mimics more real condition by adding a skin layer.

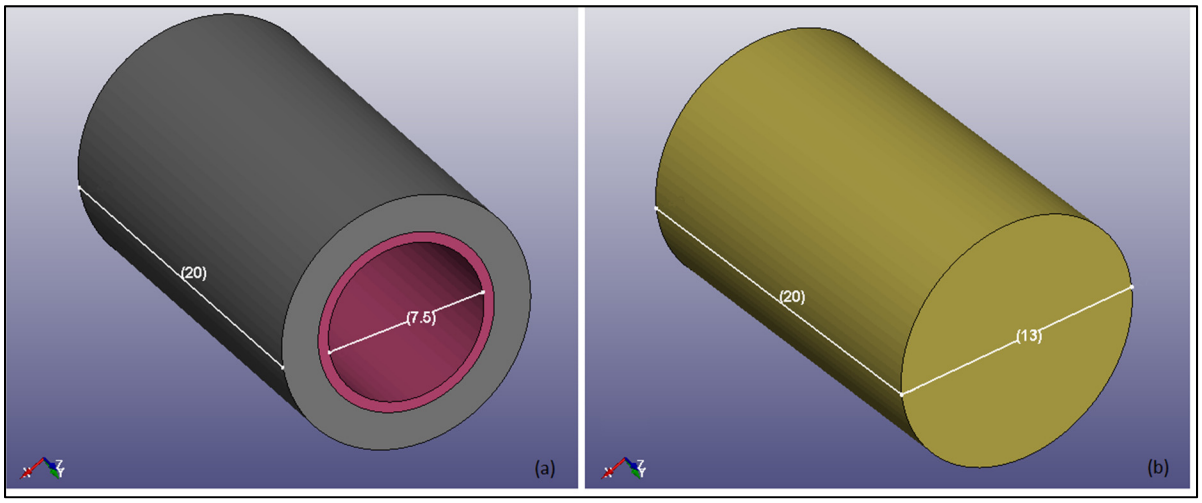

Figure 3.13 The geometry and dimensions of cylindrical earcanal with a skin layer (a) and the foam earplug (b)

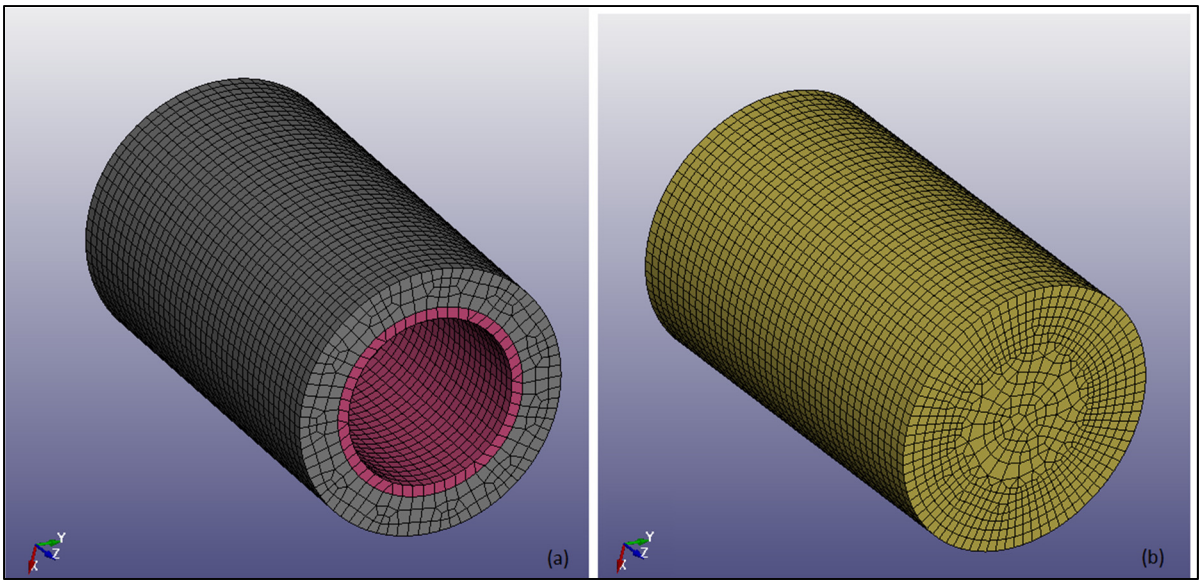

Figure 3.14 Meshed structure representing the cylindrical earcanal with a skin layer (a) and foam earplug (b)

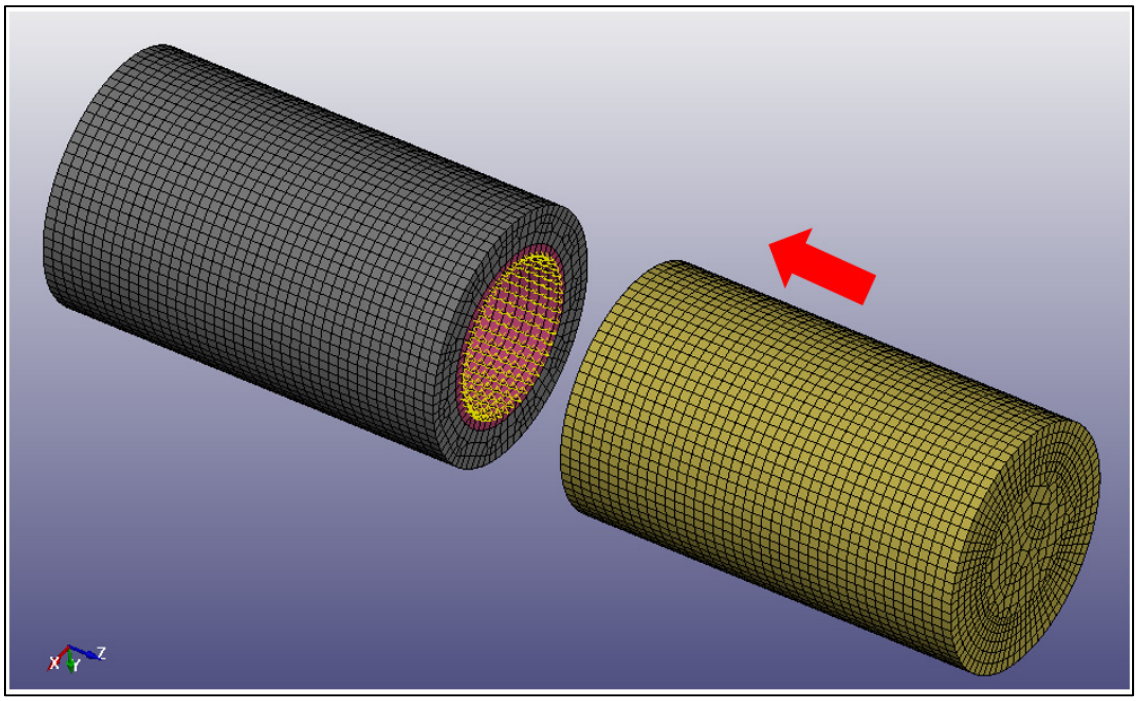

Figure 3.15 Nodes on the skin layer at the inner surface of the rigid cylinder in contact with the earplug after expansion

CHAPTER 4

RESULTS

In this chapter, results of the numerical simulations described to achieve the two specific objectives are presented.

4.1 Numerical simulation of a roll-down foam earplug under axial compression test

The material parameters obtained for K, b and n, were equal to 0.131 MPa, 13.15 and 0.022, respectively. They were obtained by a try and error method performed until a good agreement (maximum force error of 20%) was reached between the numerical and experimental force-displacement curve (Figure 4.1). It was not possible for me to improve the fit between numerical simulation and experimental curves.

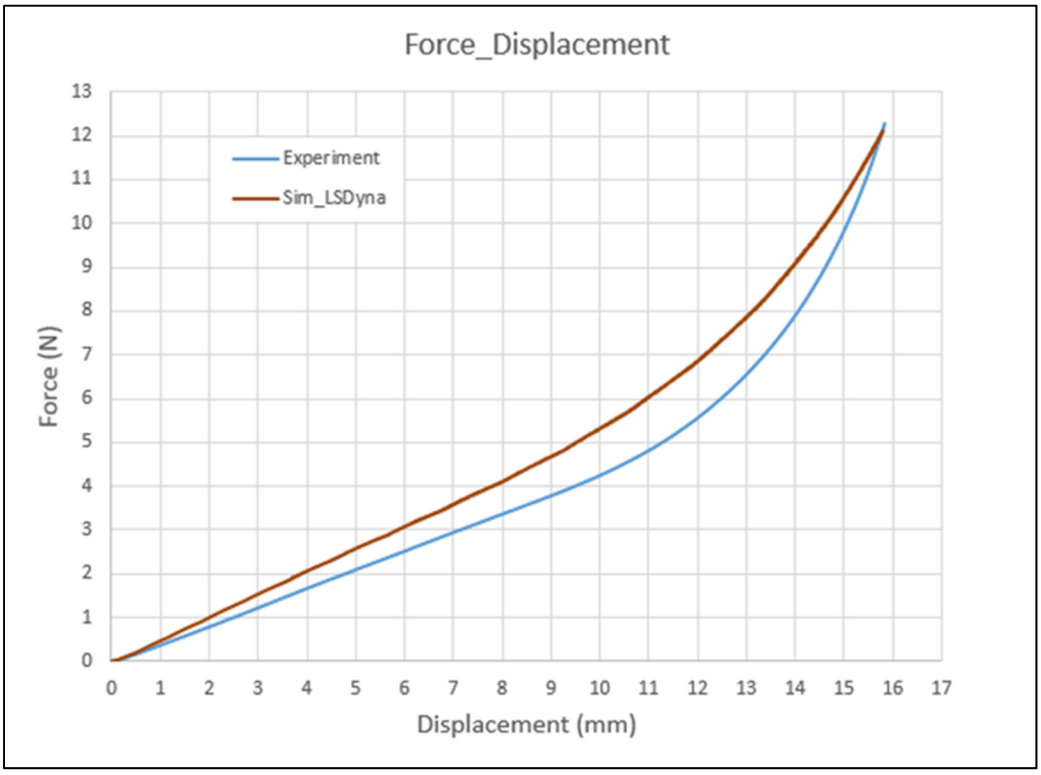

Figure 4.1 Comparison of numerical and experimental force-displacement curves for axial compression of the roll-down earplug

4.2 Numerical simulation of a roll-down foam earplug under transverse compression

By using the same material properties used in previous axial compression test for foam earplug a very good agreement in transverse compression test was obtained. They were obtained by a try and error method performed until a very good agreement was reached between the numerical and experimental force-displacement curve (Figure 4.2).

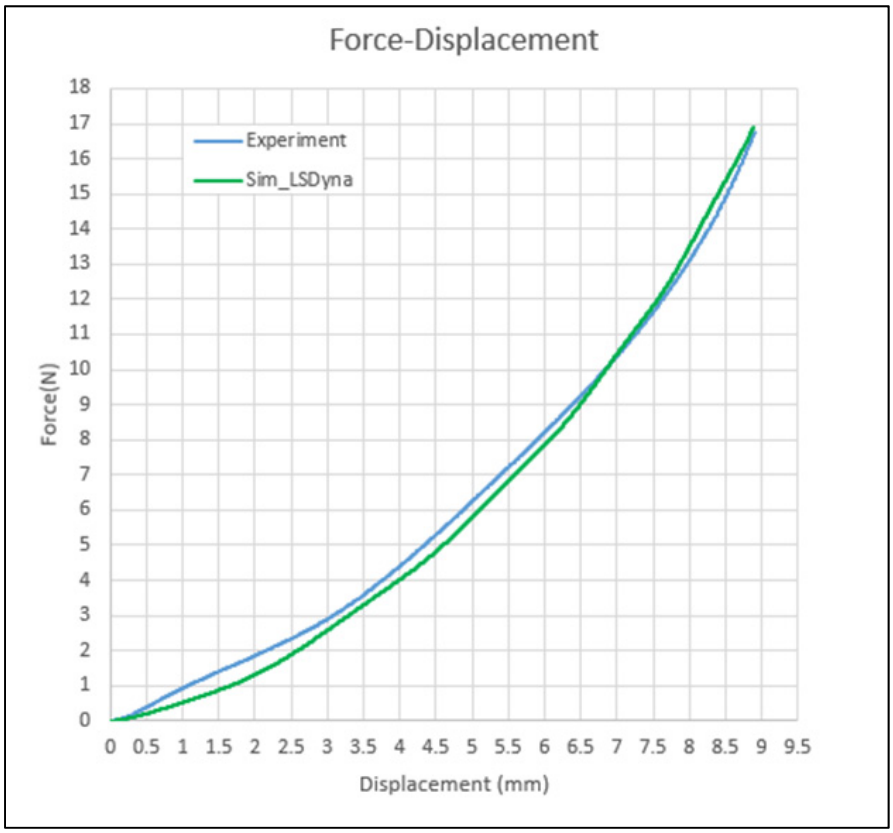

Figure 4.2 Comparison of numerical and experimental force-displacement curves for transverse compression of the roll-down earplug

4.3 Numerical Simulation of skin indentation test

The results of numerical simulations of skin indentation test (obtained by LS-Dyna) are depicted in Figure 4.3. The Von-Mises stress contour shows that the maximum stress (under indenter) is equal to 339.3 kPa at 7.5 mm indentation depth.

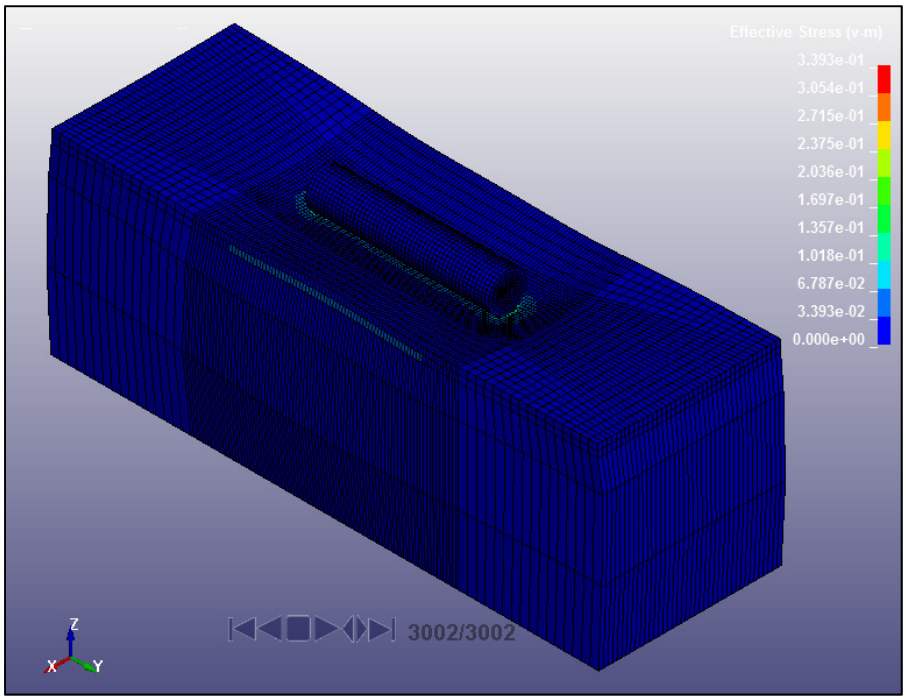

Figure 4.3 The contour of Von-Mises stress (Max: 339.3 kPa)

To compare the results of numerical simulation obtained by LS-Dyna with results of works of (Tran et. al, 2007), force-time diagram for a particular node group (summation of the 432 nodes) of the epidermis layer under the cylindrical indenter is drawn in Figure 4.4. The vertical axis shows the resultant force in Newton (N), while the horizontal axis shows the time in seconds (s). The force-time diagram shows the nonlinear hyperelastic behavior of the skin and substrate layers, where the amount of force is increased from 0 to 1.6 N during 0.3 second time (see Figure 4.4).

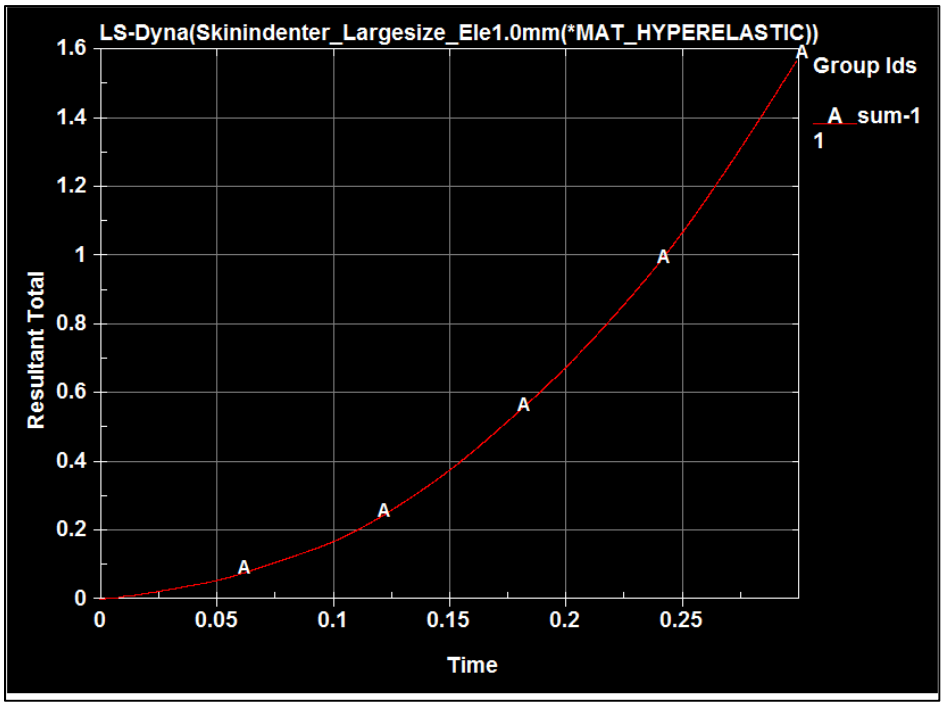

Figure 4.4 Force-time diagram during indentation of the skin and substrate layers (max force of 1.7 N at 0.3 seconds)

The force-indentation depth (force and displacement of indenter) diagram published by (Tran et. al, 2007) is depicted in Figure 4.5. The nonlinear hyperelastic behavior of skin layers obtained by numerical simulation was well correlated with his experimental works. The axial axis illustrates the force in newton (N), while the horizontal axis shows the displacement of the indenter in mm (Uy). The black square points are the experimental data, whereas red doted curve shows numerical simulation results.

The force-displacement (indentation depth) curve created by Excel 2016 for node group (summation of 432 nodes) is depicted in Figure 4.5. The result of numerical simulation was demonstrated by blue curve. This blue curve demonstrates a nonlinear hyperelastic behavior of skin and substrate layers. The amount of force was increased slightly with an increasing of the indentation depth. In more details, at 7.5 mm indentation depth, the maximum force obtained was 1.58 N in the simulation and 1.8 N in the experimentation for a difference of 11%.

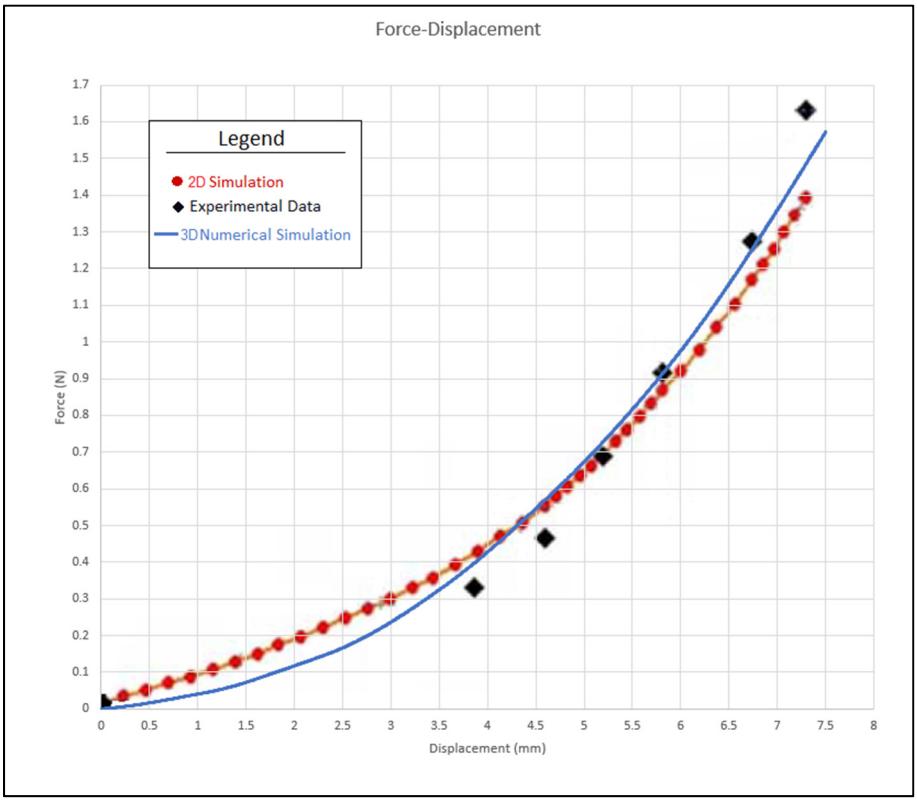

Figure 4.5 Force-displacement diagram during indentation of the skin and substrate layers (max force of 1.58 N at 7.5 mm displacement)

According to Figure 4.5, a very good correlation was evident between experimental test of (Tran et. al, 2007) and numerical simulation (blue line) obtained by LS-Dyna.

4.4 Numerical simulation and validation of the interaction of a roll-down foam earplug and a cylindrical rigid earcanal (without skin layer)

According to the first specific objective, the numerical simulation of static mechanical pressure (SMP) for a simplified cylindrical rigid earcanal was carried out while a roll-down foam earplug with larger diameter was initially compressed (rolled down) and then inserted inside a cylindrical rigid earcanal and released to expand at equilibrium.

The force-time diagram obtained from the numerical simulation is depicted in Figure 4.6. The force was obtained from nodal surface of roll-down foam earplug during numerical simulation. The vertical axis shows force values in Newton (N), whereas the horizontal axis shows time duration in seconds (s). This diagram illustrates that the force changed during compression of the foam earplug (up to a peak of 8.5 N) and its expansion after the peak. According to the red curve in this diagram, after compression and expansion, the foam earplug touches the inner surface of the cylindrical rigid earcanal (at around 75 seconds) and the contact forces remain constant at 1.6 N. The initial increasing (up to a peak of 8.5 N) and decreasing force (red curve) observed in the simulation following only compression and expansion of the foam earplug which was not observed experimentally since the load cell was fixed to cylindrical rigid earcanal and radial compression of foam earplug was done manually.

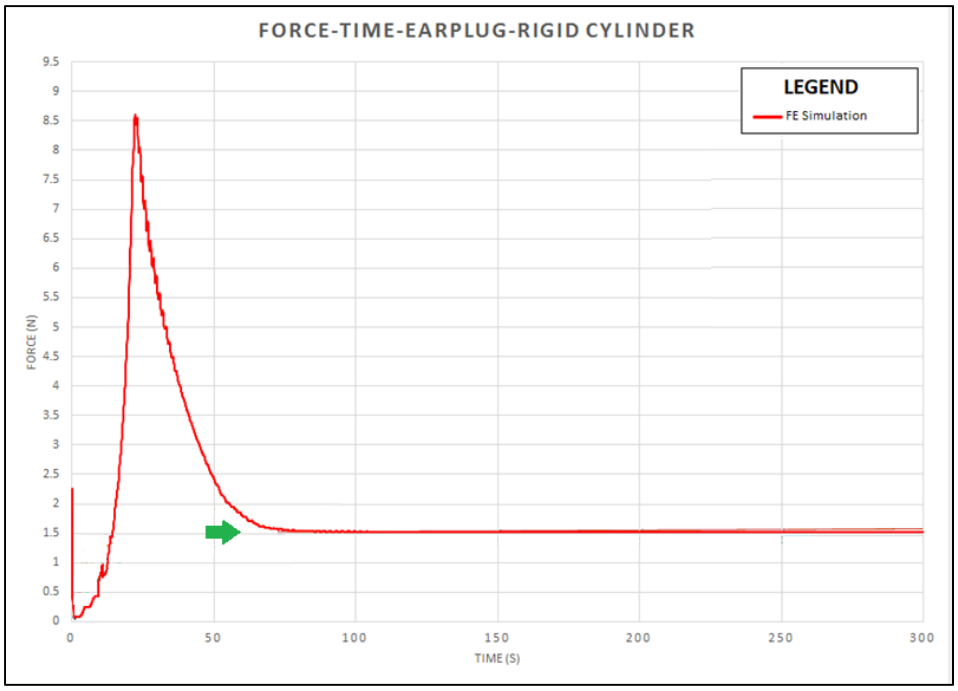

Figure 4.6 Force vs. time diagram for foam earplug compression, insertion and expansion obtained numerically

In Figure 4.7, the force-time diagram obtained from integration of the nodal forces (in radial direction) of the inner surface of the cylindrical rigid earcanal is depicted. The vertical axis shows the force in Newton (N), while the horizontal axis shows time in seconds (s). The black dotted curve shows that force at the earcanal inner surface increases after contact of the earplug (approximately 1.6 N contact forces at 80 seconds). Other curves represent the experimental force-time curves obtained by Ms. Elisabeth Laroche for different roll-down large earplugs following their expansion within a rigid cylindrical earcanal, the large earplugs and earcanal having both the same diameter as in the simulation. Results clearly show that after equilibrium, the contact force is well the experimental corridors.

As expected, the initial increasing and decreasing force depicted in the simulation result of Figure 4.6 is no longer there, as it represents the same force as the one measured experimentally. Results clearly show that after equilibrium, the contact force is well within the experimental corridors during the whole contact process.

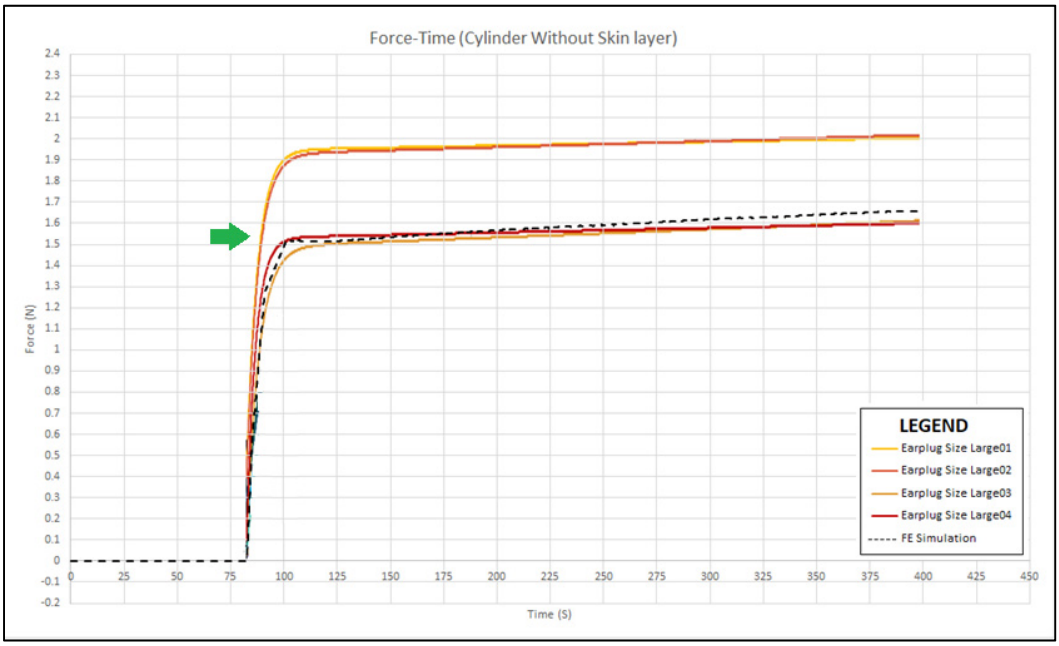

Figure 4.7 Force vs. time diagram for the earcanal inner surface nodes vs. experimental results

In order to calculate the SMP at the interface between the foam earplug and the rigid cylindrical earcanal, the area of the earcanal inner surface was calculated. The inner diameter of the cylindrical earcanal is equal to 7.5 mm. Since the length of the earcanal is equal to 20 mm, the area of the inner surface is equal to 471.23 mm² ($A_{earcanal}$):

$$A_{earcanal} = 7.5 \times \pi \times 20 = 471.23\ mm^2 \tag{4.1}$$

To calculate the SMP at the interface, the total contact force was divided by the area $A_{earcanal}$. In the numerical simulation, the contact force is equal to 1.6 N for earcanal with 7.5 mm diameter, so the total contact pressure is calculated by the following relation:

$$P_{total} = \frac{F_{average}}{A_{earcanal}} = \frac{1.6\ N}{471.23\ mm^2} = 3.395 \times 10^{-3}\ MPa = 3.395\ KPa \tag{4.2}$$

The total contact pressure (P_{total}) is equal to 3.395 kPa, which is equal to total SMP at the interface. The pressure contour at the end of the simulation is also depicted in Figure 4.8. The green color on the earplug surface illustrate that the average contact pressure was between 3.123 and 4.034 kPa, which is in agreement with the calculated SMP.

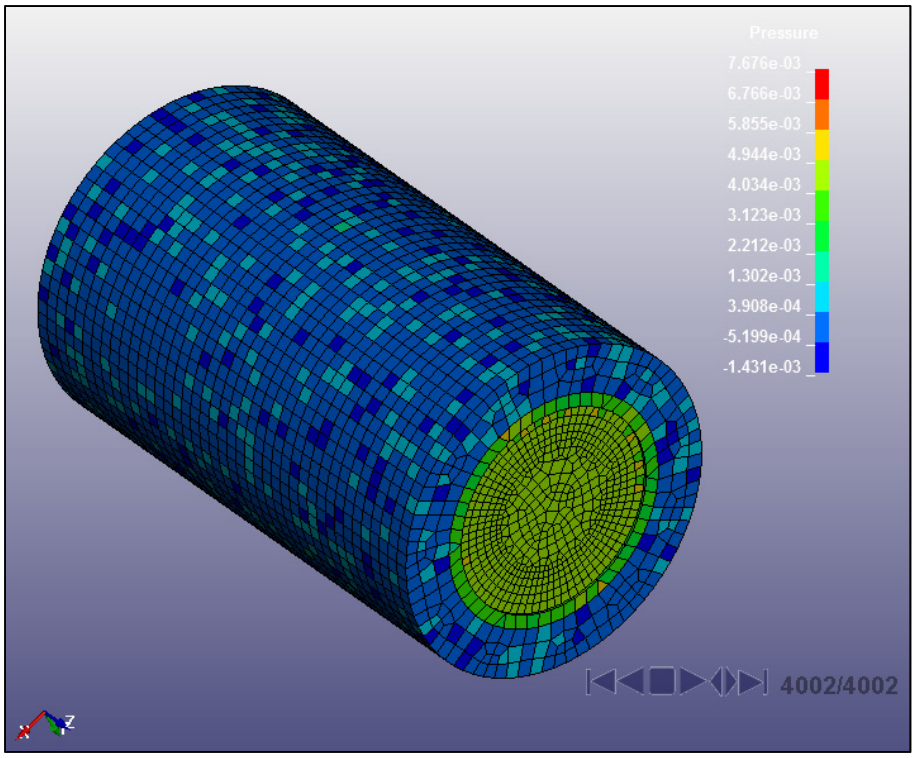

Figure 4.8 The pressure contour of the foam earplug after expansion at equilibrium (average pressure: 4.034 kPa)

4.5 Numerical simulation of the interaction of a roll-down foam earplug and a cylindrical earcanal (with a skin layer)

According to the second specific objective, a thin skin layer was added over the inner surface of the simplified cylindrical rigid earcanal. The numerical simulation of static mechanical pressure (SMP) for cylindrical earcanal with a skin layer was carried out while a roll-down foam earplug with larger diameter is initially compressed (rolled down) and then inserted inside a cylindrical earcanal and released to expand at equilibrium in the interface between the earplug and the skin layer.

The force-time diagram obtained from the numerical simulation is depicted in Figure 4.9. The vertical axis illustrates force values in Newton (N), whereas the horizontal axis shows time duration in seconds (s). This diagram illustrates that the force changed during compression of the foam earplug (up to a peak of 9 N) and its expansion after the peak. According to the red curve in this diagram, after compression and expansion, the foam

earplug touches the skin layer surface of the cylindrical rigid earcanal (at around 75 seconds) and the contact forces remains constant at 1.5 N. The Results clearly show that after equilibrium, the contact force is well within the experimental corridors. The initial increasing (up to a peak of 9 N) and decreasing force (red curve) observed in the simulation following only compression and expansion of the foam earplug which was not observed experimentally since the load cell was fixed to cylindrical rigid earcanal and radial compression of foam earplug was done manually.

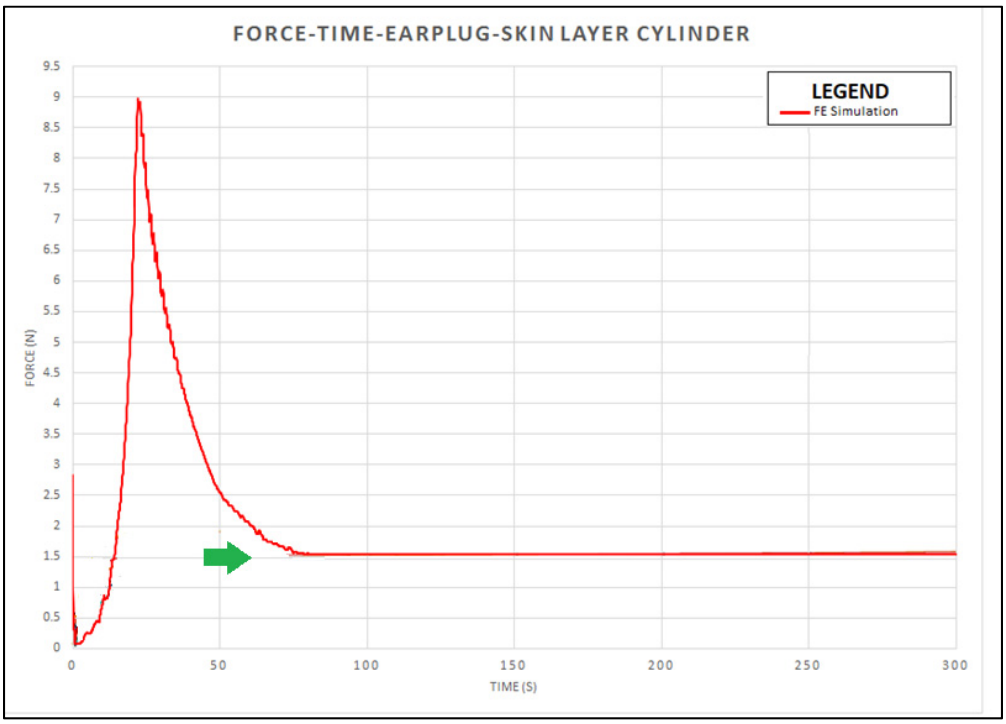

Figure 4.9 Force vs. time diagram for foam earplug compression, insertion and expansion obtained numerically

In Figure 4.10, the force-time diagram obtained from integration of the nodal forces of the skin layer inner surface inside the cylindrical earcanal is depicted. The vertical axis shows the force in Newton (N), while the horizontal axis shows time in seconds (s). The black dotted curve shows that the force at the skin layer surface increases after contact of the earplug (approximately 1.5 N contact forces at 75 seconds). Other curves represent the

experimental force-time curves obtained by Ms. Elisabeth Laroche for different roll-down large earplugs following their expansion within a rigid cylindrical earcanal, the large earplugs and earcanal having both the same diameter as in the simulation. Here the comparison was between numerical simulation of the earcanal with a skin layer and experimental test of a rigid cylindrical earcanal without a skin layer, because experimental setup with a skin layer required adding an artificial skin layer inside cavity of rigid earcanal explained in previous section. Adding an artificial skin layer inside cavity of rigid earcanal was out of scope of this master thesis.

As expected, the initial increasing and decreasing force depicted in Figure 4.9 is no longer there, as it represents the same force as the one measured experimentally. Results clearly show that after equilibrium, the contact force is well with within the experimental corridors during the whole contact process.

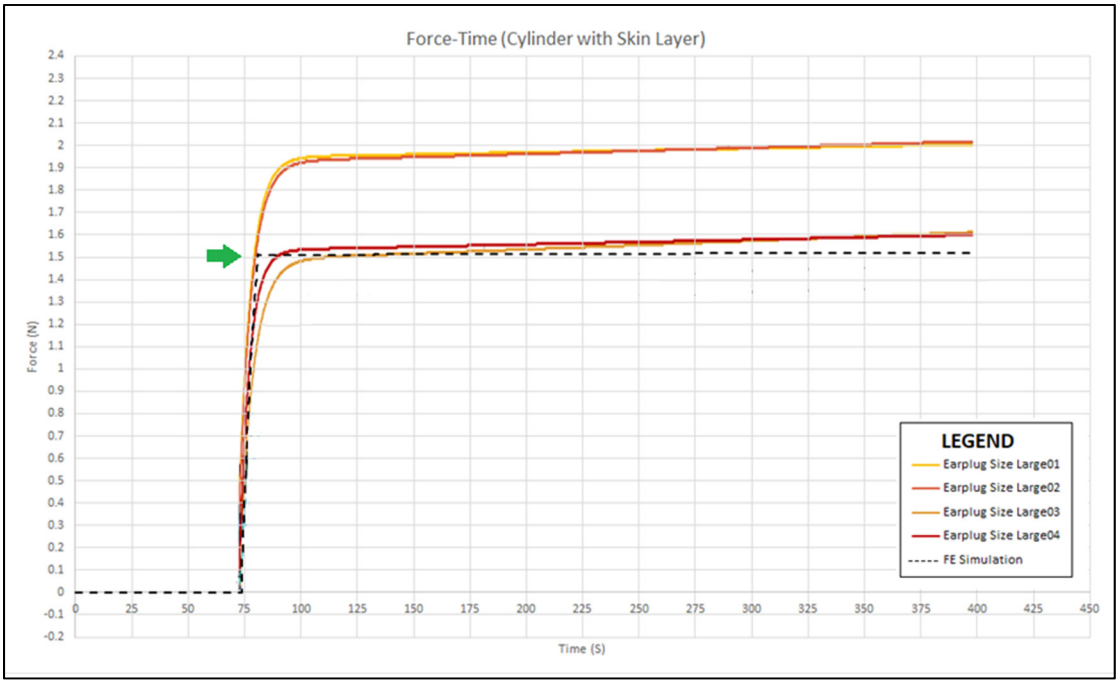

Figure 4.10 Force vs. time diagram for the skin layer surface nodes inside the earcanal vs. experimental results

In order to calculate the SMP at the interface between the foam earplug and the skin layer inside cylindrical earcanal, the area of the skin layer surface was calculated. The inner diameter of the cylindrical earcanal with a skin layer is equal to 7.5 mm. Since the length of the earcanal is equal to 20 mm, the area of the skin layer surface is equal to 471.23 mm² ($A_{skin\ layer}$):

$$A_{skin\ layer} = 7.5 \times \pi \times 20 = 471.23\ mm^2 \tag{4.3}$$

To calculate the SMP at the interface between skin layer and foam earplug, the total contact force was divided by the area $A_{skin\ layer}$. In the numerical simulation the contact force is equal to 1.5 N for earcanal with skin layer (7.5 mm diameter), so the total contact pressure is calculated by the following relation:

$$P_{total} = \frac{F_{average}}{A_{skin\ layer}} = \frac{1.5\ N}{471.23\ mm^2} = 3.183 \times 10^{-3}\ MPa = 3.183\ KPa \tag{4.4}$$

The total contact pressure (P_{total}) is equal to 3.183 kPa, which is equal to total SMP at the interface between skin layer and foam earplug.

The pressure contour at the end of simulation is also depicted in Figure 4.11. The green color on the earplug surface illustrates that the average contact pressure was between 2.347 and 4.157 kPa, which is in agreement with the calculated SMP.

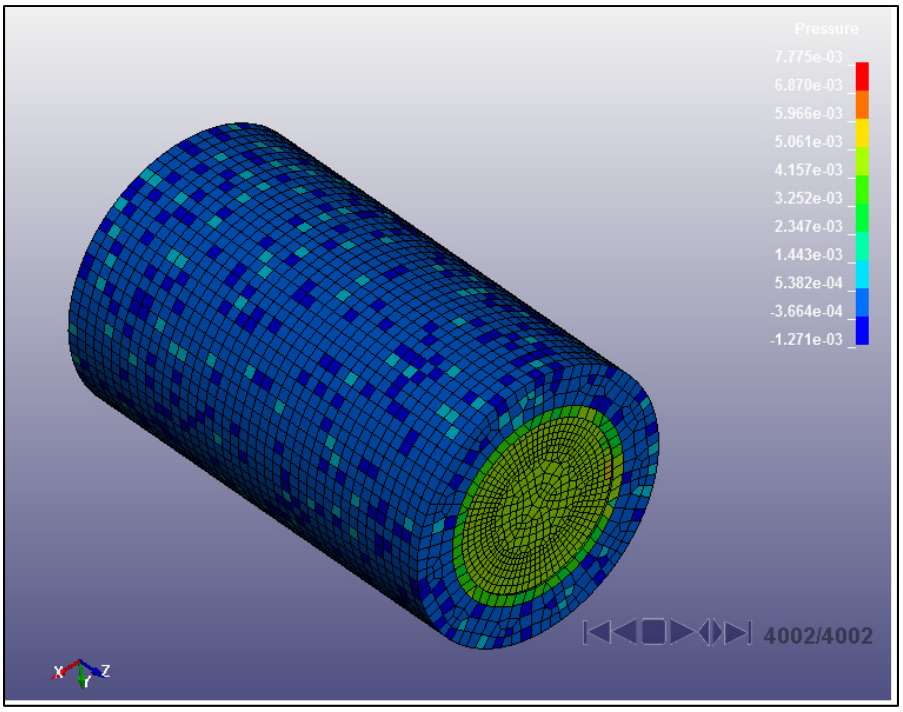

Figure 4.11 The pressure contour of the foam earplug after expansion at equilibrium (average pressure: 4.157 kPa)

In Figure 4.12, the pressure contour on the skin layer is depicted. To show pressured elements of the skin layer at the interface, the earplug geometry was hidden. The green color on the skin layer surface illustrates that the average contact pressure was between 2.347 and 4.157 kPa, which is in agreement with the calculated SMP.

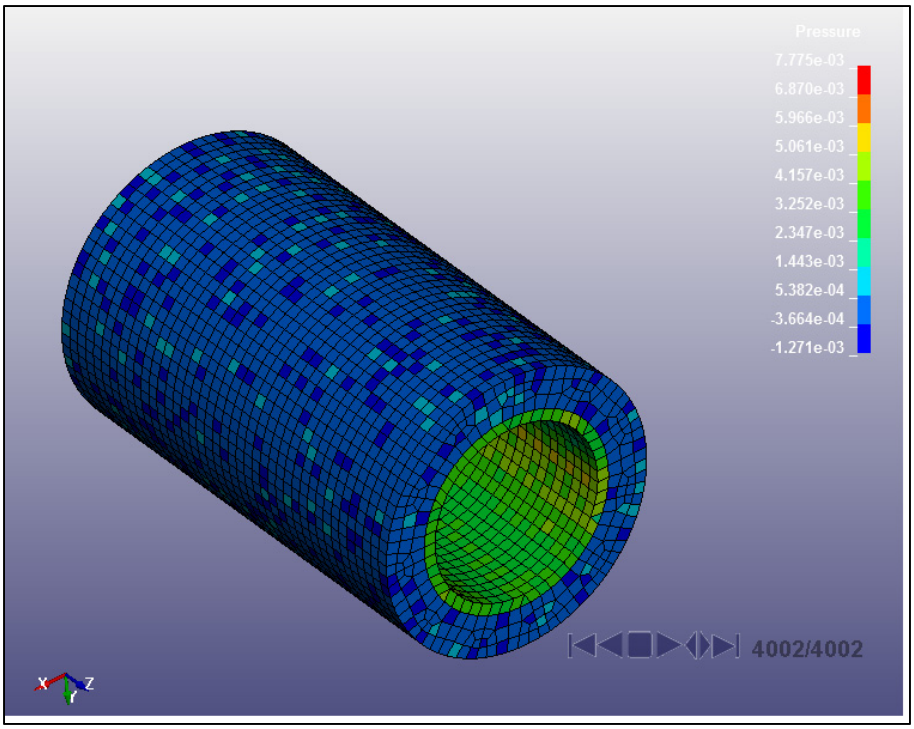

Figure 4.12 The pressure contour of the skin layer inside at equilibrium (average pressure: 4.157 kPa)

CHAPTER 5

DISCUSSION

In this chapter, the originality of the method used for SMP calculation and the obtained results, as well as its limitations are discussed.

Currently, there is no test bench to measure the SMP at the interface between a foam earplug and a human earcanal. The numerical simulation is thus employed as a tool to predict the SMP exerted by a foam earplug on a human earcanal. The originality of this project is that not only we can predict the SMP using a simplified FEM, but we can also partly verify the SMP results using experiments. The proposed work of (Baker et. al, 2010) was a very good example to predict the SMP at the interface between earplugs and earcanal wall. Although, they could achieve good results to predict the SMP, they considered human skin material model as a simple elastic material. In our work, we considered human skin material model as a hyperelastic material to mimic more realistic human skin behavior. Moreover, they did not characterize foam earplug mechanical properties, however we characterize material model of roll-down foam earplug as a hyperelastic model which represented much closer material behavior to real foam earplug.

The proposed work of (Tran et. al, 2007) was unique to characterize the mechanical properties of the human skin layer, because he worked on an *in-vivo* project, not on post-mortem human subject (cadaver). His numerical simulation results were matched with obtained experimental data. However, our numerical simulation results had a much better correlation with their experimental data. One reason for our better accuracy was most probably the use of a 3D model. Although, numerical simulation in 3D is more demanding and is time consuming, it obviously can better catch the intrinsic geometrical particularity of a deformed shape following indentation. In other words, our numerical simulation results were much closer to the real experimental work of (Tran et. al, 2007). The second reason of the better accuracy of our numerical simulation is that a refine mesh was employed on all skin layers under the indenter, and played a key role to increase the accuracy of our

numerical simulation. The third reason of a better accuracy of our numerical simulation is the type of boundary conditions applied for FE modeling of skin layers. In this work, the finite elements of skin layers were merged together, similar to the real human skin layers. Node by node merge system causes reduction of error in convergence of results as well as an increasing in the accuracy of the numerical simulation. In fact, the amount of force on all nodes under the indenter was distributed equally on each skin layer.

The characterization of the mechanical properties of a roll-down foam earplug is a giant challenge, due to the open and close cells of the foam earplug structure and its viscous behavior. To characterize these mechanical properties, two different compression tests were reproduced by finite element in this project. An axial and a transverse compression tests were used to characterize mechanical properties such as Young modulus, shear modulus and bulk modulus using trial-and-error method. Radial compression test of a roll-down earplug would have been more realistic than axial and transverse compression tests, as it is closer to our application. In our work, the viscoelastic behavioral law was neglected. However, a hyperelastic material model was an appropriate material model since it allowed reproducing the nonlinear behavior of roll-down foam earplugs while the effect of time was negligible.

The numerical simulation of axial compression test of a roll-down foam earplug is demanding, because in the experimental test, the earplug was compressed to 60% of its height, from 20 mm to 4 mm. This large strain is related to the material and the microstructure of the earplug with open air cells. Numerical simulation of large strain is significantly difficult, because large strain causes instability and convergence error in FE simulation. Moreover, the penetration of foam earplug elements in both top surface and basement is inevitable. To prevent abovementioned problems, selection of an appropriate contact algorithm was the key. At the end, the results of the numerical simulations were correlated with experimental data in both axial and transverse compressions. Although, the results of axial compression test demonstrated mismatch between numerical simulation and experimental data, the results of transverse compression test illustrated a much less mismatch between numerical simulation and experimental data. One reason of mismatch between

numerical simulation and experimental data in axial compression test might be a larger strain during numerical simulation with respect to transverse compression test.

The numerical simulation of foam earplug expansion inside a cylindrical rigid earcanal can be used to predict the contact pressure value at the interface between both parts, which is equal to the SMP. In order to perform such numerical simulation, the use of appropriate boundary conditions plays a vital role. The boundary conditions should be similar to real conditions to mimic foam earplug radial compression and expansion. In other words, an initial radial compression should be induced on foam earplug before insertion inside cylindrical earcanal and then compressed earplug should be inserted inside cylindrical earcanal, then the radial compression should be deactivated causes earplug to be relaxed and finally earplug expands to touch cylindrical earcanal wall. Uniform radial compression of foam earplug is a special loading case that involves large deformation and required a particular method. The expansion time, after insertion of the earplug inside the cylindrical earcanal, was similar to real condition (approximately 1 minute). The contact force of 1.6 N at the interface at equilibrium in the numerical simulation was well within the experimental corridor. Similarly, the contact force value was equal to 1.5 N when a skin layer was added. The SMP (i.e. contact pressure) at the interface between foam earplug and the rigid cylindrical earcanal without a skin layer and with a skin layer were 3.395 kPa and 3.183 kPa, respectively. However, these aforementioned SMP values were much less compared with other literature such as works of (Baker et. al, 2010). The proposed works of (Baker et. al, 2010) demonstrated the SMP between 25 kPa and 50 kPa. One reason for this dissimilarity could be the simplification of the material models of the human skin and the foam earplug in proposed works of (Baker et. al, 2010). He mentioned a soft foam earplug but with a hard plastic part at the end of soft part. Furthermore, he compressed only the material of 20% during characterization process. He also investigated a 3D model of earcanal with complex geometry.

There are some limitations for the measurement and prediction of the SMP. Currently, there is not appropriate flexible pressure sensor to measure the SMP inside a human earcanal. Existing pressure sensors are too bulky to insert into a small canal with a diameter of

approximately 7.5 mm. The geometry of the human earcanal is very complex, so simplification of earcanal to a cylindrical canal helped us to predict the SMP at the interface between a roll-down foam earplug and an earcanal. The repetition of works of (Smith et. al, 1982) by Ms. Elisabeth Laroche, helped us to understand and measure contact force at the interface between foam earplug and rigid cylindrical earcanal. The experimental data from works of Ms. Elisabeth Laroche is validated by numerical simulation.

The characterization of mechanical properties of skin layers inside human earcanal is another demand. There is not any device to measure mechanical properties of earcanal skin. In this project we proposed that the human skin mechanical properties of earcanal were similar to the epidermis skin layer of the forearm, as the one measured in (Tran et. al, 2007). This proposal cannot be validated until the time that a device appears in market to directly measure the mechanical properties of the human earcanal skin.

CONCLUSION AND PERSPECTIVES

No test bench is currently available to measure the SMP at the interface between a foam earplug and a human earcanal. As a consequence, a FE simulation was used as a tool to predict the SMP exerted by a roll-down foam earplug on a human earcanal. The originality of this project is that not only we can predict the SMP but we can also verify the FEM by using experimental data. There are many obstacles to measure the SMP inside the human earcanal, notably the small size and the complex shape of the earcanal. Thus simplification of the geometry of the earcanal was an appropriate approach to take this global project one step further. Another simplification was to consider that the mechanical properties of the human skin layer in the forearm was similar to those of the skin layers inside the human earcanal.

The specific objectives, which aimed at building finite element models (FEM) with two levels of complexity to compute the SMP, were met. A first model that simulated the insertion of a roll-down foam earplug (3M classic E.A.R made of PVC foam) in a simplified cylindrical rigid earcanal without skin was built and validated, and a second model that simulated the insertion of the foam earplug in a more realistic earcanal that includes a skin layer was built. To reach those objectives, the mechanical behavior of the human skin and foam earplug were characterized experimentally in complementary studies and used to derive proper mechanical properties for both FEM. The characterized mechanical properties of human skin and foam earplug were validated by using numerical simulation (FEM). The geometry of foam earplug and simplified earcanal were acquired before earplug insertion.

The mechanical properties of foam earplug were characterized by using experimental tests. The foam earplug was compressed in two axial (along its height) and transverse (along its diameter) directions by using a mechanical testing device (MTS Systems & Corporation). Following calibration of the earplug material properties, the finite element modeling provided similar to force-displacement curves than the experimental compression tests.
The material model hyperelastic (highly compressible) is used to simulate behavior of foam earplug, which is based on strain energy function defined by (Hill et al, 1979) and (Storakers

et al, 1986). To compare results of numerical simulation with experimental tests data, numerical simulation results were correlated with the obtained data of experimental tests. The force-displacement curves obtained from experimental compression tests and numerical simulations were evaluated. A very good correlation was obtained from results of transverse compression test in both experimental and numerical simulation. However, comparison between data of experimental test and numerical simulation was resulted a mismatch in force-displacement curves obtained from axial compression test. The main reason of this mismatch was the large strain deformation during axial compression test of foam earplug in numerical simulation. Generally, large stain deformation causes convergence error in numerical simulation.

The indentation test is a dominant test method to characterize mechanical properties of human skin. The mechanical properties of human skin layers were characterized by (Tran et. al, 2007). However, the forearm skin shown different mechanical properties with respect to skin of human earcanal, the possible way was to assume similar behavior laws for the skin of the earcanal. The hyperelastic material behavioral laws of four layers were considered as nonlinear Neo-Hookean slightly compressible material model (homogeneous and isotropic). The numerical simulation of indentation test carried on in 3D similar to experimental test of (Tran et. al, 2007). The force-displacement curve of experimental data of (Tran et. al, 2007) was correlated with obtained curve from numerical simulation. The properties of skin layers were identified so that the error between the experiment and the model was minimal. The obtained curve showed a very good match with experimental data. The dominant reasons for appropriate results in numerical simulation were boundary conditions in 3D, refined finite elements under indenter, contact algorithm and precision of LS-Dyna software. The convergence study approved the precision of LS-Dyna software.

The contact force between roll-down foam earplug and rigid cylindrical earcanal is measured by experimental test by Ms. Elisabeth Laroche. The force-time diagrams for expansion of roll-down foam earplug inside rigid cylindrical earcanal were obtained from experimental tests. According to objective 1, the numerical simulations were carried out to mimic

experimental tests. To validate obtained results of numerical simulation, the force-time curves of experimental tests were compared with numerical simulations. The contact forces were computed at the interface between the roll-down foam earplug and the rigid cylindrical earcanal without skin layer. The contact force was 1.6 N at the interface. According to objective 2, a much more complex proposal was defined by adding a skin layer (epidermis) inside rigid cylindrical earcanal. The contact forces were calculated at the interface between the roll-down foam earplug and the epidermis layer inside the rigid cylindrical earcanal. The contact force was slightly less (1.5 N) at the interface. The SMP (i.e. contact pressure) at the interface between the roll-down foam earplug and rigid cylindrical earcanal without the epidermis layer was 3.395 kPa and with the epidermis layer was 3.183 kPa. Due to the fact that the epidermis layer was reduced the SMP at the interface. Although, the objective 1 was validated by experimental test, the objective 2 was not validated by experimental test due to some limitations.

There is a lot of perspective to this work:

- The geometry of earcanal is very complex (“S” form and ducky shape), and its dimension is very small to insert flexible pressure sensor. The available flexible sensors are bulky and cannot be inserted inside an earcanal. Finding appropriate flexible pressure sensors for insertion inside an earcanal can be considered an important progress to directly measure the SMP.

- The mechanical properties of the skin layers inside the earcanal are unknown. The mechanical properties of human skin are different for each body part. An appropriate device to characterize mechanical properties of human earcanal *in vivo* is not available, because human earcanal has small dimensions and measurement test may not be suitable ethically. Figuring out the mechanical properties of the human skin earcanal would be very useful to better predict the SMP.

- The viscoelastic behavior of foam earplug was neglected in this project. Although, the mechanical properties of foam earplug were characterized in some publications, those results were might not be fully appropriate to predict the SMP. The viscoelastic behaviors of foam earplug may play a significant role to predict the SMP.

- Wearing roll-down foam earplug requires radial compression of the earplug before insertion. Thus, radial compression test would provide more appropriate results for the mechanical properties of the foam earplug than transverse and axial compression tests. Carrying out a test bench is required to compress foam earplug radially. Consideration of radial compression test results will improve the obtained values of the SMP prediction.

APPENDIX I

A.1 Convergence of results of the FEM used for foam transverse compression test

An analytical model was used to prove convergence of the numerical simulation that replicate transverse compression test of foam earplug. The analytical model was implemented by MATLAB. In Figure A.1 shows a comparison of both the FEM (element size of 1 and 5 mm) and the analytical model. The vertical axis shows force over the Young's modulus multiplied by length and time. The horizontal axis illustrates delta time over whole of time. The blue curve shows the result of the analytical model while the yellow and purple curves show numerical simulation results.

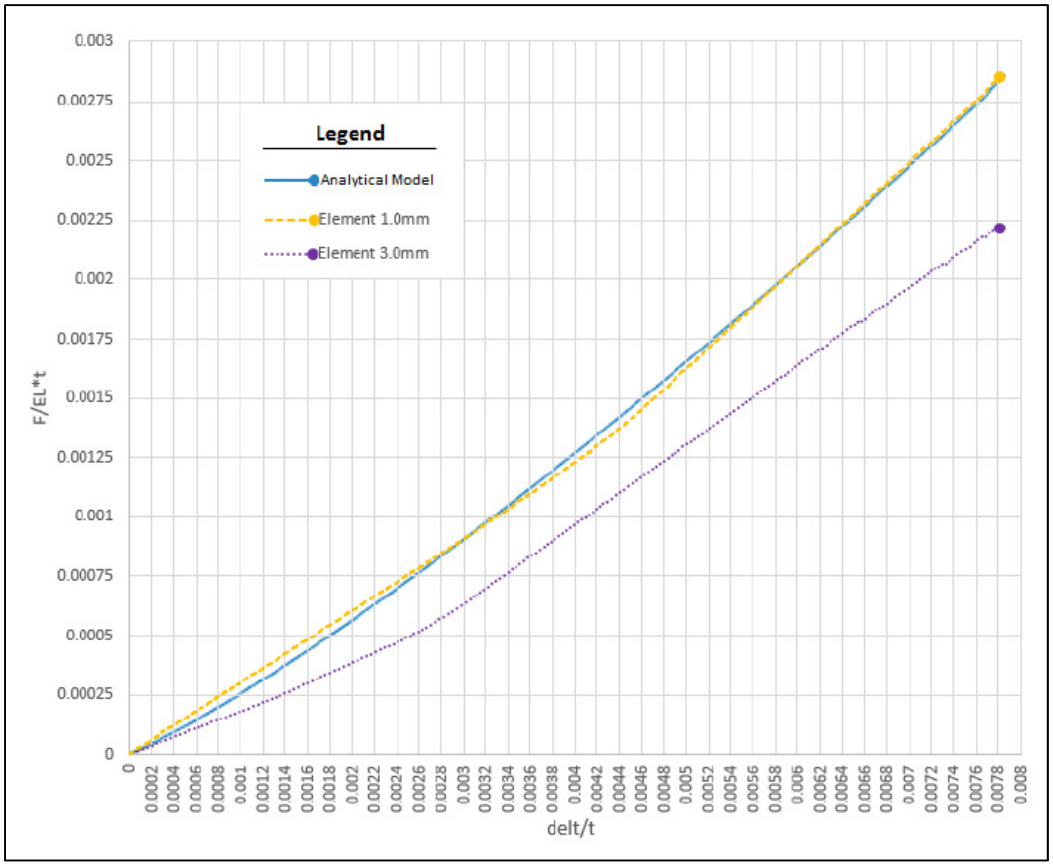

Figure I.1 Comparison between the FEM and an analytical model that mimics the transverse compression test

Increasing the number of elements (element size 1.0 mm) causes better a better match between the analytical and numerical results, thus showing that use of element size of 1.0 mm was required to appropriately represent the compression test.

A.2 Convergence of results of the FEM used for skin indentation

In order to evaluate the convergence of the FEM used to replicate the skin indentation test, the obtained indentation force is presented as a function of the size of the elements (Figure A.2). When, the element size is decreased, the number of elements under the indenter is increased. The number of elements for each numerical simulation is increased until to reach a plataue.

The horizontal axis shows the number of elements of the epidermis area under the indenter (from 90 to 3840 elements), whereas the vertical axis shows summation of nodal forces over the epidermis surface in each numerical simulation.

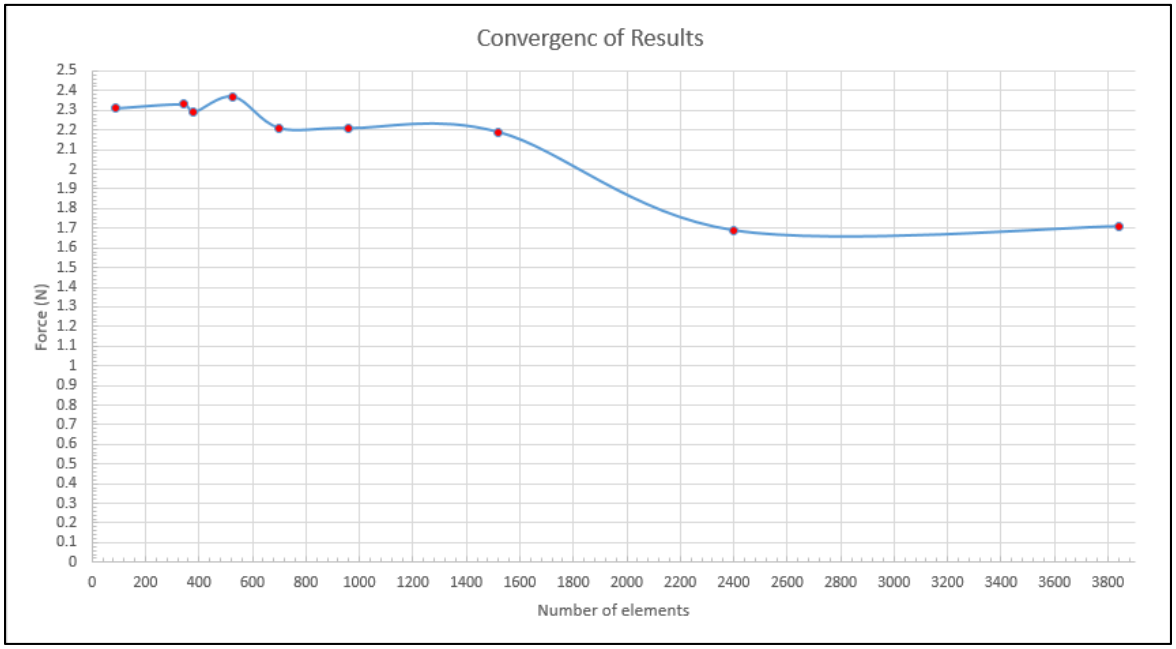

Figure I.2 Diagram of the convergence of the Force (N) vs. Number of elements

LIST OF BIBLIOGRAPHICAL REFERENCES

Agache, P., G., Monneur, C., Leveque, J., L., & Rigal, J., D., (1980). "Mechanical Properties and Yong's Modulus of Human Skin", Arch Dermatol Res 269, 221-232.

Albin, T. & Engineers, A., (2007). "A Pressing Question-How Much Contact Pressure Is Too Much?", 10thApplied Ergonomics Conference.

Baker, A., T., Lee, S., H., & Mayfield, F. (2010). "Evaluating Hearing Protection Comfort through Computer Modeling", Kimberly-Clark Corporation, SIMULIA Customer Conference.

Benacchio, S., Varoqaux, A., Wagnac, É., Doutres, O., Callot, V., Bendahan, D., & Sgard, F., (2016). "Ear Canal Deformations by Various Earplugs: An Insitu Investigation using MRI".

Benacchio, S., Doutres, O., Le Troter, A., Varoquaux, A., Wagnac, E., Callot, V., & Sgard, F., (2018). "Estimation of the Ear Canal Displacement Field Due to In-ear Device Insertion using a Registration Method on Human-like Artificial Ear", Hearing Research, 365, 16-27.

Berger, E. H., Royster, L., H., Royster, J., D., Driscoll, D., P., & Layne, M., (2003). "Noise Control and Hearing conservation: why do it?", The Noise Manual, American Industrial Hygiene Association.

Berger, E., H., (2011). "Custom Hearing Protection Have it Your Way … Maybe", Issue of Industrial Hygiene News.

Bhattacharya, S., K., Tripathi, S., R., & Kashyap, S., K., (1993). "Assessment of comfort of various hearing protection devices", J Hum Ergol, 22, 163-72.

Bischoff, J., E., Arruda, E., M., & Grosh, K., (2000). "Finite Element Modeling of Human Skin using an Isotropic Nonlinear Elastic Constitutive Model", The Journal Biomechanics 33, 645- 652.

Brummund, M., K., Sgard, F., Petit, Y., & Laville, F., (2014). "Three-dimensional Finite Element Modeling of the Human External Ear: Simulation Study of the Bone Conduction Occlusion Effect", The Journal of the Acoustical Society of America 135, 1433.

Carioli, J., Delnavaz, A., Zednik, R. J., Voix, J., (2016). "Power Capacity from Earcanal Dynamic Motion", American Institute of Physics (AIP) Advances 6, 125108.

Carioli, J., Delnavaz A., Zednik, R., J., & Voix, J., (2018). “Piezoelectric Ear canal Bending Sensor”, IEEE SENSORS JOURNAL, Vol. 18, No. 5.

Casali, J., G., Lam, S., T., & Epps, B., W., (1987). “Rating and ranking methods for hearing protector wearability”, Sound Vibration, 21:10-8.

Che, H., Nigg, B., M., & de Konig, J., (1994). “Relationship between plantar pressure distribution under the foot and insole”, Clinical Biomechanics, Vol. 9, Issue 6, 335-341.

Cobb, T., K., Cooney, W., P., & An, K., N., (1995). “Pressure Dynamics of the carpal tunnel and flexor compartment of the forearm”, The journal of Hand Surgery, Vol. 20, Issue 2, pp. 193-198.

Daly, C. H. & Odland, G., F., (1979). “Age-related Changes in the Mechanical Properties of Human Skin”, the Journal of Investigative Dermatology, 73:84-87.

Darkner, S., Larsen, R., & Paulsen, R., R., (2007). “Analysis of Deformation of the Human Ear and Canal Caused by Mandibular Movement”, MICCAI, LNCS 4792.

Davis, R., R., & others, (2008). “What do we know about hearing protector comfort?”, National Institute for Occupational Safety and Health (NIOSH), Noise and Health, 10 (40) , p. 83.

Delalleau, A., Josse, G., Lagarde, J., M., Zahouani, H., & Bergheau, J., M., (2006). “Characterization of the mechanical properties of skin by inverse analysis combined with the indentation test”, Journal of Biomechanics, 39, 1603-1610.

Delalleau, A., Josse, G., Lagarde, J., M., Zahouani, H., & Bergheau, J., M., (2008). “Characterization of the mechanical properties of skin by inverse analysis combined with an extensometry test”, WEAR, 264, 405-410.

Diridollou, S., Berson, M., Vabre, V., Black, D., Karlsson, B., Auriol, F., Gregoire, J., M., Yvon, Vaillant, C., L., Gall, Y., & Patat, F., (1998). “An invivo Method for Measuring the Mechanical Properties of the Skin using Ultrasound”, Ultrasound in Med & Biol., Vol. 24, No. 2. pp. 215-224.

Diridollou, S., Vabre, V., Berson, M., Vaillant, L., Black, D. Lagarde, J., M., Gregoire, J., M., Gall, Y., & Patat, F., (2001). “Skin Ageing: Changes of Physical Properties of Human Skin in vivo”, International Journal of Cosmetic Science, 23, 353-362.

Dufour, F., (2015). “Persons with hearing loss in workplace”, Employer Support Services.

Fligor, B., (2013). “Variability in pressure applied to the ear canal during silicone impressions and digital scanning,” Lantos Technologies.

Fransson-Hall, C., & Kilbom, A., (1993). “Sensitivity of the hand to surface pressure”, Applied Ergonomics, 24 (3), pp. 181-189.

Gardner, Jr., R., & Stoughton, M., (1974). “Earplug Composed of Polymeric Foam Materials”, US Patent 3811437.

Gardner, Jr., R., & Stoughton, M., (1977). “Earplug Composed of Polymeric Foam Materials”, US Patent 29487.

Gardner, R., Jr., Laroche, M., B., (1992). “Polymeric Foam Earplug”, International Application Published under the Patent Cooperation Treaty (PCT), WO 92/06659.

Gerges, S., N., Y., & Casali, J., G., (2007). “Chapter 31.Hearing Protectors”, Handbook of Noise and Vibration Control, Crocker, Malcolm j., PP. 367-376.

Grenness, M., J., Osborn, J. & Lee Weller, W., (2002). “Mapping ear canal movement using area-based surface matching”, The Journal of the Acoustical Society of America 111, 960.

Guilhem, V., & Voix, J., (2016). “Custom Molded Silicone Earplugs: Effect of Material Properties on Acoustic Attenuation and Mechanical Skin Contact”, Candaian Acoustics, Vol. 44, No.3, 161.

Hendriks, F., M., Brokken, D., van Eemeren, J., T., W., M., Oomens, C., W., J., Baaijens, F., P., T., & Horsten, B., A., M., (2003). “A numerical-experimental method to characterize the non-linear mechanical behavior of human skin”, Skin Research and Technology, 9, 274-283.

Herman, I., P., (2016). “Physics of the Human Body.”, The Biological and Medical Physics, Biomedical Engineering, p.247.

Hsiao, H., Guan, J., & Weatherly, M., (2002). “Accuracy and precision of two in-shoe pressure measurement”, Ergonomics, Vol. 45, No. 8, 537-555.

Ivarsson, A., Toremalm, N., G., & Brühl, P., (1990). “Eczema, itching, heat and humidity problems-Impediments to the effective use of hearing protectors”, Proceedings of Internoise, Göteborg, Sweden: Institute of Noise Control Engineering, pp. 1093–1096.

Jian, M., Xia, K., Wang, Q., Yin, Z., Wang, H., Wang, C., Xie, H., Zhang, M., & Zhang, Y., (2017). “Flexible and highly sensitive pressure sensors based on bionic hierarchical structures”, Advance Functional Materials, 27, 1606066.

Kim, H., Hong, S., Jang, N., Ha, S., Lee, H. & Kim, J. (2017). “Wearable resistive pressure sensor based on highly flexible carbon composite conductors with irregular surface morphology”, ACS Applied Materials and Interfaces, 9, 17499-17507.

Kim, J., H., & Kadam P., (2004). “Measurement of Earplug extraction force for various ear plug-ear canal combinations”, University of Cincinnati, USA.

Kramer, R., K., Majidi, C., & Wood, R., J., (2011). “Wearable tactile keypad with stretchable artificial skin”, Robotics and Automation (ICRA), 2011 IEEE International Conference on, IEEE, pp. 1103-1107.

Kunov, H., Abel, S., M., & Giguere, C., (1986). “An acoustic test fixture for use with hearing protective devices”, report 8SE84-00241, the department of national defence, Downsview, Ontario, Canada.

Kunov, H., Racansky, D., & Ing, A., (1988). “Simulated intra-aural skin for an artificial ear”, report W7711-6-9280/01-SE, the department of national defence, Downsview, Ontario, Canada.

Kuijt-Evers, L. F. M., Bosch, T., Huysmans, M. A., de Looze, M. P. & Vink, P., (2007). “Association between objective and subjective measurements of comfort and discomfort”, Applied Ergonomics, Vol. 38, Issue 5, 643-654.

Lampe, W., R., (1972). “Room Temperature Vulcanizable Silicone Rubber Composition”, US Patent, 3,696,090, Serial No. 76,265.

Langlois, C., Panneton, R., & Atalla, N., (2001). “Polynomial relations for quasi-static mechanical characterization of isotropic poroelastic materials”, Journal of Acoustical Society of America, Vol. 110, No.6.

Maguet, D., Croisier, J., L., Demoulin, C., & Crielaard, J. M., (2004). “Pressure pain thresholds of tender point sites in patients with fibromyalgia and in healthy controls”, European Journal of Pain 8, pp. 111-117.

Manschot, J., F., M., & Brakkee, A., J., M., (1986). “The Measurement and Modelling of the Mechanical Properties of Human Skin in vivo”, Journal of Biomechanics, Vol. 19, No. 7. pp.511-515.

Maroonroge, S., Emanuel, C. D., & Letowski, T., R., (2000). “Basic Anatomy of the Hearing System.”, usaarl.army.mil.

Marvi-Mashhadi, M., Lopes, C., S., & Llorca, J., (2018). “Effect of Anisotropy on Mechanical Properties of Polyurethane Foams: An experimental and Numerical Study”, Mechanics of Materials 124, 143-154.

Mecanum, QMA, (2016). “Quasi-static Mechanical Analyzer”, Model: QMA, Installation and Instruction Manual, Revision.

National Institute of Health, (2016). “Noise-Induced Hearing Loss”, National Institute on Deafness and Other Communication Disorders (NIDCD) Fact sheet.

Norris, J., Chambers, R., Kattamis, N., Davis, B., & Bieszczad, J., (2012). “Effects of Custom Earplug Design Parameters on Achieved Attenuation”, Creare Inc. www.creare.com.

Pailler-Mattei, C., Bec, S., & Zahouani, H., (2008). “In vivo measurements of the elastic mechanical properties of human skin by indentation tests”, Medical Engineering and Physics, 30, 599-606.

Paris, M, (2018). “Mapping the cutaneous sensitivity of the auditory canal human”, Master thesis, École de Technologie Supérieure (ETS).

Park, J., Lee, Y., Hong, J., Ha, M., Do Jung, Y., Lim, H., Youb Kim, S., & Ko, H., (2014). “Giant tunneling piezoresistance of composite elastomers with interlocked microdome arrays for ultra sensitive and multimodel electronic skins”, ACSNANO, Vol. 8, No. 5, 4689-4697.

Park, M., Y., & Casali, J., G., (1991). “An empirical study of comfort afforded by various hearing protection devices: Laboratory versus field results”, Appl Acousti, 34: 151-79.

Pereira, J., M., Mansour, J., M., & Davis, B., R., (1991). “Dynamic Measurement of the viscoelastic properties of skin”, The Journal Biomechanics Vol. 24, No. 2. pp. 157-162.

Potts, R., O., Cherisman, D., A., Jr., & Buras, E., M. Jr., (1983). “The Dynamic Mechanical Properties of Human Skin in vivo”, Journal of Biomechanics, Vol. 16, No. 6. pp.365-372.

Qi, L., Liu, H., Justyn W., Funnel R., J., & Daniel, S., J., (2006) “A Nonlinear Finite-element Model of the Newborn Ear canal”, The Journal of the Acoustical Society of America, 120, 3789.

Rampel, D., Evanoff, B., Amadio, P., C., de Krom, M., Franklin, G., Franzblau, A., Gray, R., Gerr, F., Hagberg, M., Hales, T ., Katz, J., N., & Pransky, G., (1998). “Consensus Criteria for the Classification of Carpel Tunnel Syndrome in Epidemiologic Studies”, American Journal of Public Health, 88, pp.1447-1451.

Sangeorzan, B., J., Harrington, R., M., Wyss, C., R., Czerniecki, J., M., & Matsen III F., A., (1989). "Circulatory and mechanical response of skin to loading.", Journal of Orthopaedic Research, 7: 425-431.

Santoni, C., B., & Fiorini, A., C., (2010). "Pop-rock musicians: assessment of their satisfaction provided by hearing protectors", Brazilian Journal of Otorhinolaynology, 76 (4), pp. 454-461.

Schulz, G., Rublack, K., Meister, A., Dybowski, S., Dubrau, KH., & Gretzschel, D., (1983). "Comparative studies of insulting effect and the wearing properties of hearing protector means at the place of employment", Z Gesamte Hyg Ihre Grenzgeb, 29:93-8.

Schwartz, G., et al., (2013). "Flexible Poltmer transistors with high pressure sensitivity for application in electronic skin and high monitoring", Nature Communications, 4, p. 1859.

Silver, F., H., Freeman, J., W., & DeVore, D., (2001). "Viscoelastic Properties of Human Skin and Processed Dermis", Skin Research and Technology, 7, 18-23.

Smith, C., R., Broughton, R., M., Wilmoth, J., N., Borton, T., E., & Mozo, B. T., (1982). "Physical Characteriscs and Attenuation of Foam Earplugs", American Industrial Hygiene Association Journal, (43) 1/82.

Staab, W., J., Sjursen, W., Preves, D., & Squeglia, T., (2000). "A one-size disposable hearing aid is introduced", The Hearing Journal, vol. 53, pp. 36–38.

Staab, W., J., Ph.D., (1996). "The Philips XP peritympanic Hearing aid", Seminars in Hearing, Vol. 17.

Staab, W., "2016. Ear Impression History-The slow death of powder and liquid", https://hearinghealthmatters.org/waynesworld/2016/powder-liquid-ear-impression-slowdeath/.

Stewart, R., D., (1959). "Ear Protector", US Patent, 2,910,980, Serial No. 660,277.

Stinson, M., R, & Lawton, B., W., (1989). "Specification of the Geometry of the Human Ear Canal for the Prediction of Sound-Pressure Level Distribution", the Journal of the Acoustical Society of America, 85, 2492.

Tran, V., Charleux, F., Rachik, M., Ehrlacher, A., & Hobatho, M., C., (2008). "In vivo Characterization of the Mechanical Properties of Human Skin and Passive Muscle", Journal of Biomechanics, Volume 41, 16th Congress European Society of Biomechanics, p. S29.

Tran, H., V., Charleux, F., Rachik, M., Ehrlacher, A., & Ho Ba Tho, M., C., (2007). "In Vivo Characterization of the Mechanical Properties of Human Skin Derived from MRI and Indentation Techniques", Computer Methods in Biomechanics and Biomedical Engineering, ISSN: 1025-5842.

Viallet, G., Sgard, F., Laville, F., & Boutin, J., (2014). "A finite element model to predict the sound attenuation of earplugs in an acoustical test fixture", Journal of the Acoustical society of America, Vol. 136, issue 3.

Voix, J., (2014). "Did you Say Bionic Ear", Universite du Quebec (ETS), Montreal, QC, H3C1K3.

Vronda, D., R., & Westmann, R., A., (1970). "Mechanical characterization of skin-finite deformation", The Journal Biomechanics Vol. 3, pp. 111-124.

Wheeler, D., E., & Glorig, A., (1956). "The Industrial Hygienist and Ear Protection," Noise Control, vol. 2, pp. 45–72.

Xu, F., Li, X., Shi, Y., Li, L., Wang, W., He, L., & Liu, R., (2018). "Recent developments for flexible pressure sensors: A review", Micromechanics, 9, 580.

Zwislocki, J., (1958). "Ear Protection: Effectiveness vs. Comfort", Bioacoustic laboratory, Syracuse, New York, Acoustic Society of America, Noise Control 4, 1.